# ICE RUBBLE IMPACT WITH A MOORED PLATFORM

by

W.A. Nixon and R. Ettema

IIHR Limited Distribution Report No. 147

Prepared for

Hitachi Zosen Corporation
Osaka, Japan

Mobil Research and Development Corporation
Dallas, Texas

U.S. Department of the Interior Minerals Management Service
Washington, D.C.

Iowa Institute of Hydraulic Research
The University of Iowa
Iowa City, Iowa 52242-1585

April 1988

TABLE OF CONTENTS

**ABSTRACT**

Thirty two tests have been performed to determine forces associated with rubble ice moving against a model cable-moored platform, using the IIHR ice towing tank facility. The rubble ice was formed by freezing sheets of urea-doped ice to the appropriate thickness (5 or 25mm) and then breaking up these sheets using a pushblade on the motorized carriage. The broken ice was stored under insulation while further sheets were grown. For the tests, the rubble ice was spread into layers 5, 50 and 100mm thick.

The model platform was free to surge, heave and pitch. Restoring forces in the surge direction were provided by a leaf spring designed to simulate a cable mooring system. Restoring forces for heave and pitch resulted from the platform's buoyancy.

The rubble ice was pushed past the platform at velocity of 0.02, 0.04, 0.10 or 0.20m/s. Typical behavior involved the formation of an accumulation of rubble ice, or "ice prow," at the leading edge of the platform, which would slough off periodically and jam between the platform and the side of the tank. To avoid this problem, a series of tests were conducted in which the platform was towed through the ice, thus avoiding the "jamming."

For both the towed and stationary model, ice forces against the platform increased monotonically with rubble-layer thickness. The effect on ice forces of velocity was less clear, with surge and heave forces showing apparent maxima with ice velocity. Platform pitch angle remained essentially constant with ice velocity, within the accuracy obtainable due to experimental scatter.

## ACKNOWLEDGEMENTS

The authors with to thank Dr. M. Matsuishi of Hitachi Zosen Corporation, Dr. R. Johnson of Mobil Research and Development Corporation and Mr. C. Smith of U.S. Minerals Management Service for their guidance in conduct of this project. Additionally, the authors wish to thank Mr. S. Iwata of Hitachi Zosen Corporation for assisting in conduct of the experiments.

## EXTENDED ABSTRACT

Cable-moored platforms have considerable potential both as exploration and production platforms in relatively deep (100 feet or greater) Arctic offshore waters. One of the ice conditions which such platforms will encounter is fields of ice rubble. This study was undertaken to examine the forces exerted on a cable-moored platform by rubble ice.

The tests were conducted at The University of Iowa's Institute of Hydraulic Research (IIHR) using the ice towing tank there. The model tested was a 1/45-scale model, somewhat similar in shape to the "Kulluk" platform. The rubble ice was made from 0.7% urea solution ice sheets either 5mm thick or 25mm thick. The ice sheets were broken into uniform rubble mechanically and stored under polystyrene sheets until sufficient rubble had been accumulated.

The platform was free to heave, pitch and surge [while being restrained from rolling, yawing, or swaying), with restoring forces being provided by buoyancy in the case of heave and pitch, and by a leaf spring in the case of the surge motion. The stiffness of the leaf spring (0.5 kN/m) was chosen to be similar to the mooring stiffness used on the "Kulluk" platform.

Tests were performed for three layer thicknesses of rubble ice (single layer thick, 50mm, 100mm) and at four impact speeds (0.02, 0.04, 0.1 and 0.2m/s).

In the initial series of tests, the rubble ice was pushed past the platform. Previous work (Matsuishi and Ettema, 1985a) indicated the formation of a stable "prow" of ice, but in these tests no such stable "prow" formed. Rather, a "prow" would start to form, then slough off to the side, causing a jamming process to occur between tank and platform. To avoid this phenomenon, which was not felt to be representative, a number of tests were performed in which the platform was towed through the ice.

Mean and peak values of heave and surge force increased monotonically as the layer thickness increased, as did the peak pitch values. The mean pitch values decreased for the thickest ice layer. Surge and heave both appear to show a maximum with velocity, which possibly results from resonance effects, while the peak values of pitch were apparently constant with ice velocity.

In all cases, heave displacement and surge force were greater for the towed platform than for the stationary case. This arises, at least in part, from the added mass of the moving platform and also from boundary effects arising from the side of the tank.

## LIST OF FIGURES

## LIST OF TABLES

# I. INTRODUCTION

A moored platform in ice-covered waters is likely to be impacted by fields of moving ice rubble. This is especially true when ice-breaking ships are extensively used to manage and break ice around the structure, as was the standard operating procedure for the moored platform "Kulluk" (Hnatiuk and Wright, 1984; Loh and Stamberg, 1984; Pilkington et al., 1986). Prediction of ice loads resulting from moored platform interaction with fields of ice rubble is complex because load magnitudes are governed by unpredictable patterns of ice-rubble accumulation around the platform and by platform motions during impact. In turn, patterns of ice-rubble accumulation, and platform motions, are influenced by rubble field thickness, size distribution of constituent rubble ice, and by speed of rubble-field impact.

## A. Scope of the Study

This study is intended to extend the work reported by Matsuishi and Ettema (1985a). They measured the load response and motions of both a moored and a fixed test platform of conical hull shape somewhat similar to that of "Kulluk." The test platform (see figure 1) had a waterline diameter of 1.5 m, and its conical shape flared to a cylindrical skirt of diameter 1.0 m, which lines the bottom of the platform and is designed to protect the mooring cables for such a platform from direct impact with the ice (see figure 2).

In contrast with the study by Matsuishi and Ettema, in this study only a "moored" platform was tested, and the mooring spring stiffness was different from that used by Matsuishi and Ettema. Also, the ice rubble was of different sizes, being produced from sheets 5 and 25mm thick, as opposed to the 30-millimeter-thick, and much weaker (20kPa, flexural strength), sheets used by Matsuishi and Ettema.

## B. Previous Work

Relatively little work has been published on ice loads exerted against inverted conical structures, especially loads resulting from moving fields of rubble ice. Ralston (1980) and Milano (1980, 1982) presented analytical models for determining ice-sheet loads against conical structures, whi1st Frederking (1980), Frederking and Schwarz (1982) and Wessels (1984) performed scale-model tests to determine ice loads against conical structures. Matsui-shi and Ettema (1985a,b) performed tests, using the moored platform used in this study, to determine loads due to both rubble ice and ice floes. Further work on ice loads exerted against moored platforms in moving sheet ice is given in Nixon and Ettema (1987), a companion to this report. A more extensive review of the literature concerning ice-sheet loading of structures is given in Matsuishi and Ettema (1985b).

Hellmann (1984) reports the results of small-scale tests conducted with a conical body thrust through enclosed ice rubble. Although the loading condition in his experiments was not fully similar to that of the present study, his data generally reveal some similar trends to those observed in it. Other related studies, dealing with ship hulls amidst ice rubble, were conducted by Ettema et al. (1985), Greisman (1981) and Mellor (1980). As in the present study, Ettema et al. examined the influence of rubble size on resistance (or horizontal force) and showed that layers comprising larger ice-rubble pieces generally produced larger resistance forces.

## C. Equations of Motion of a Floating Moored Platform

The genera1 form of the equation of motion for a floating moored platform can be expressed as:

$$\underset{(i)}{[M]}\{\ddot{x}\} + \underset{(ii)}{[C]}\{\dot{x}\} + \underset{(iii)}{[K]}\{x\} = \underset{(iv)}{\{F\}} \tag{1}$$

where term (i) relates to platform inertia, term (ii) to damping, term (iii) to mooring and buoyant restoring forces and moments, and term (iv) to ice forces and moments. Bearing in mind that a moored platform has six degrees of freedom, and referring to figure 9 for axes, we have:

$$\{x\} = \begin{Bmatrix} x \\ y \\ z \\ \theta_x \\ \theta_y \\ \theta_z \end{Bmatrix} \tag{2}$$

where x, y, and z are heave, surge and sway, respectively; and $\theta_x$, $\theta_y$, and $\theta_z$ are yaw, roll and pitch, respectively. The force vector {F} is given as

$$\{F\} = \begin{Bmatrix} F_x \\ F_y \\ F_z \\ M_x \\ M_y \\ M_z \end{Bmatrix} = \begin{Bmatrix} \int_A p_x dA \\ \int_A p_y dA \\ \int_A p_z dA \\ \int_A (p_y \ell_y - p_z \ell_z)\, dA \\ \int_A (p_z \ell_z - p_x \ell_x)\, dA \\ \int_A (p_x \ell_x - p_y \ell_y)\, dA \end{Bmatrix} \tag{3}$$

where $p_x$, $p_y$, $p_z$ are the pressures in the x,y,z directions; A is the contact area between the rubble ice and the platform; and $l_x, l_y, l_z$ are moment arms associated with orthogonal lines of action of ice pressure against the hull.

Note that shear and friction forces between ice and hull have been neglected in this representation. In freezing brash ice, for instance, such an assumption may be invalid.

As discussed below, for these tests z, $\theta_x$ and $\theta_Y$ were constrained to be zero. Similarly, through x and $\theta_z$ were measured directly, y was inferred by means of measuring, with a load cell, the restoring force exerted by the leaf spring in the mooring harness.

## II. EXPERIMENTAL PROCEDURE

### A. Test Facilities

#### 1. IIHR Ice Towing Tank

Experiments were conducted using the IIHR ice towing tank which is 20m long by 5m wide by 1.3m deep (see figure 3). Ice sheets can be grown on it at a maximum thickening rate of 2.0mm per hour.

A motorized carriage (see figure 4) was used either to push the ice rubble against the platform (done in two series of tests) or to pull the platform through the rubble ice (done in one test series). The carriage can move at velocities between 0.001 and 1.50m/s. Velocity is measured by means of a photo-detector and a wheel with regularly space holes mounted on the shaft.

#### 2. The Test Platform

The test platform is similar to the existing cable-moored platform "Kulluk" at 1:45 scale. Principal dimensions of both "Kulluk" and the test platform are given in Table 1, while figure 5 shows a detailed drawing of the test platform.

A floating cable-moored platform can be considered affected by three linear restoring forces or moments (Matsuishi and Ettema, 1985b):

(a) A horizontal mooring force, modeled in this case by means of a linear leaf spring with stiffness $K_s$ = 0.5kN/m.

(b) A vertical foundation reaction force due to buoyancy; $K_h$ = 17.3N/m.

(c) A foundation reaction moment again due to buoyancy; $K_p$ = 35.1kNm/degree.

## 3. Instrumentation

As noted above, the platform was attached in two different ways; either to the carriage, from which it was towed, or to the instrument beam. However, in both cases the instrumentation of the platform was the same.

The platform was connected to either the beam or the carriage by way of a linear mooring harness and a load cell (a 490-Newton NISHO DENKI LMC-3502-50 load cell) as shown in figure 6. The mooring harness (see figure 7) comprised a pair of elastic leaf springs, a spline bearing, stroke bearings and universal bearings. Yawing and swaying of the platform were restricted by two vertical rods located fore and aft on the platform. As shown in figure 8, the rods were constrained to slide in slots. Thus, the platform had three degrees of freedom for motion; heave, pitch and surge.

Heave and pitch motions were measured by means of two linear voltage displacement transducers (LVDT's), which sensed the vertical motion of the platform at two positions, fore and aft. The LVDT's were excited using 12

volts with a full stroke range of 0.15m.

Locations of the measuring sensors and the positive directions of recorded data are shown in figure 9. The output voltages were scanned with a digital voltmeter and then serially transmitted to the IIHR HP-1000E computer system for disc storage. Data acquisition bandwidth was 120Hz, though each channel was sampled at a rate of either 7 or 10Hz.

## 4. Transducer Calibration

For each of the data-logging transducers, the zero level and sensitivity were determined before each test.

The load cell output voltage, v, was measured for an amplifier-created calibration strain $\varepsilon_c$. The sensitivity, S, of the load cell was evaluated as

$$S = (v/\varepsilon_c)\, C \qquad (4)$$

where C is a predetermined ratio of strain to the force experienced by the transducers.

Sensitivities of the LVDT's were evaluated by measuring the voltage change for a given displacement of the transducer rod. The sensitivity of the carriage velocity measurement was determined by correlating the output voltage with the mean carriage velocity as measured with a length scale and stop watch. Table 2 lists the calibration coefficients.

B. Model Ice Rubble

The growth of the ice rubble sheets was a two stage process. First, an unseeded sheet was grown from a 0.7% urea solution to the desired thickness (either 5 or 25mm). This sheet was then broken up by an attachment on the push-blade of the towing carriage and, by use of screens, stored under insulation at one end of the tank. This process was repeated until between 7 and 10 sheets had been grown. At this point, sufficient ice had been collected for testing. The ice was then spread over the tank surface to the required layer thickness. Three thicknesses of rubble layer were tested; single layer, 50mm layer and 100mm layer. Between tests, the layer was carefully groomed to achieve again a uniform thickness. Table 3 gives the rubble size distribution and layer porosities. Mean and standard deviation of two size distributions. Porosity of each layer ≃ 0.36.

C. Test Procedure

A total of 32 tests were performed of which 13 were with the platform towed by the carriage. All of these latter tests were for 5-millimeter-thick rubble ice. The tests in which the platform was attached to the instrument beam used both 5 and 25mm thick ice. The impact velocities used were 0.2, 0.1, 0.04 and 0.02m/s.

## III. PRESENTATION OF RESULTS

A Data

Individual time series from the tests are presented in a separate addendum to this report. The data obtained from the digital voltmeter was converted, by means of a simple computer program, to "engineering" values (N for

force, mm for heave, degrees for pitch). The time histories were also analyzed to give the temporal mean, standard deviation about the mean, and maximum and minimum values for the variable. The mean was taken only for the period in which steady state was achieved. Table 4 gives the results for the tests in which the platform was attached to the instrument beam, while table 5 gives the results for those tests in which the platform was towed by the carriage.

B. Stationary Platform

Figures 11 through 14 show the variation of surge force, heave displacement and pitch angle with impact speed for the platform attached to the instrument beam. Note that, following the practice of Matsuishi and Ettema (1985b), mean values and mean values plus two standard deviations are plotted. The latter is intended to indicate maximum value of a measured quantity; e.g., of force.

For rubble formed of the 5-millimeter-thick ice, surge force appears (figures 10a, lla, and 12a) to show a maximum at ice impact speeds of between 0.05 and 0.10m/s. Heave (figures 10b, llb and 12b) also shows a maximum in the same velocity range. Pitch data (figure 10c) exhibit some scatter and, while there is a similar maximum for the 100mm layer, no such maximum is obvious for the 5 and 50mm layers. Conversely, for the 25-millimeter-thick ice, in a single layer, surge force and heave increase mildly with increasing speed. The pitch data, though suggesting a maximum of pitch at ~ 0.20m/s, show negligible variation with speed. The occurence of maximal mooring force can be attributed to congestion of rubble ice between the platform and the tank walls. As mentioned earlier, such congestion developed because ice prows

that formed at the leading perimeter of the platform sloughed towards its sides becoming congested between the platform and the tank walls. The congestion effectively placed the platform amidst a thickened layer of rubble and lead to increased ice forces being exerted against the platform. The congestion of rubble ice was greatest for the speed range of 0.02 to 0.10m/s. At lower speeds, creeping speeds, false-bows remained stable at the leading perimeter of the platform. For speeds higher than this range, false-bows were sufficiently diminished in size that their influence on ice forces decreased.

Figures 15 through 18 show the variation of surge force, heave and pitch with layer thickness for the 5-millimeter-thick ice. In all cases, surge force and heave increase monotonically with increasing layer thickness. For impact velocities of 0.02 and 0.10m/s there is an obvious upward curve to the data, which is not clearly present for velocities of 0.04 and 0.20m/s. For the pitch data, the increase of peak values with layer thickness is apparent for velocities up to 0.10m/s, though the mean values do not show this increase, at the 100mm layer thickness. However, for ice impact velocity of 0.20m/s pitch angle shows a maximum for both peak and mean values.

### C. Towed Platform

Figures 19 through 21 show the variation of heave, surge force and pitch with ice speed for those tests in which the platform was towed through the ice by the carriage.

Figures 22 through 24 show heave, pitch and surge force, respectively, as functions of ice layer thickness. Again, at the three velocities shown (0.04, 0.10, 0.20m/s) surge force and heave increase monotonically with layer

thickness, though no upward curvature is apparent in this case. Scatter in the data obscures any trends of pitch with layer thickness. However, peak values at 0.10 and 0.20m/s show clear monotonic increases, while the mean values drop off at the 100mm thickness.

### D. Visual Records

Video tape recordings were made of all tests viewing the impact zone between ice rubble and platform. Underwater video recordings were also made of many tests, again viewing the impact zone. After each test, the bottom of the platform was swept clean and any ice under there was photographed after the sweeping process.

## IV. DISCUSSION

### A. Qualitative Observations

It was expected that, as the ice moved against the platform, a stable and stationary cone of ice would form as a "false-bow" at the platform's leading perimeter. And, as a consequence of this, surge force, heave and pitch would all increase until a stable cone had formed, at which point they would remain essentially constant. This expectation was based on the observations of Matsuishi and Ettema (1985a). However, rather than a cone achieving stability, ice cones would form and grow, then slough-off to one side. Often the sloughed off cone would jam between the side of the tank and the platform, adding considerably to the force subsequently exerted against the platform by the blocked advancing rubble field. In effect, this "sloughing" behavior, combined with the confinement of the tank sides, transformed the rubble field to a pressurized rubble field. However, this may reflect nature in that as a

rubble field flows around a structure the "far field" of the rubble field effectively provides a degree of confinement. In other words, in nature, a rubble field provides to some extent its own confinement.

### B. Towed versus Stationary Platfonn

In an attempt to avoid the confinement discussed above it was decided to perform a series of experiments in which the platform was towed through the ice. This of course does not model nature, as significant water currents occur around the platform. But the hope was that in this way the jamming that had been observed when the platform was attached to the beam could be avoided, since it was felt this jamming was not reflective of nature either. The expectation then, was that the towed platform would experience a lower surge force (also heave and pitch) than the platform attached to the beam. However, the opposite was observed. In all cases heave was greater for the towed platform. Pitch was approximately equal in the two cases, if anything, slightly greater in the towed experiments. Surge force was definitely greater in the towed experiments for the 5 and 50-millimeter-thick layers.

The higher forces and motions experienced in towed experiments, over against the stationary experiments, arise from the manner in which the mean and peak values are obtained for the stationary tests. As can be seen in figure 25, the surge forces on the towed platform rose to a plateau and then remained essentially constant. In contrast, see figure 26, for the stationary platform the force reached an initial plateau (corresponding to dormation of a stable "false-bow") but then rose to much higher values as the "false-bow" sloughed off and jammed against the side of the tank. As this latter process was considered "unnatural," mean and peak values for the stationary platform

were taken from the initial plateau. Values for the towed platform are higher than the stationary platform values because of added mass effects.

### C. Mean and Peak Values

Matsuishi and Ettema (1985a) noted that the variation of surge force and heave with ice thickness were essentially linear. A similar result is found here. Matsuishi and Ettema (1985a) also noted that the pitch changed sense with increasing ice thickness and also became more scattered (i.e., the standard deviation increased significantly). While the pitch angle did not change direction in these experiments, the mean value did decrease at the highest layer thickness, and the standard deviation at that condition was considerably greater than for the other layer thickness. Matsuishi and Ettema (1985a) suggested this effect arises from a change in pressure distribution (from the ice) as a result of a different layer thickness. The results observed here do not contradict this explanation.

The apparent maximum observed in surge force as a function of ice velocity may be an artefact of experimental scatter. However, the fact that the maximum shifted to a higher velocity for the larger (25mm thick) ice pieces raises the possibility of some resonance effect. Further experimental work is needed to elucidate this point. However, from Table 6 (which shows the natural period of oscillation and the logarithmic decrement of the platform for pitch, heave and surge), in combination with Table 3 which shows characteristic lengths, $l_c$, of the ice rubble pieces, it may be possible to provide a rationale for the maximum. On average we would expect a new piece of ice to impact the platform every $t$ seconds where:

$$t = \frac{l_c}{V} \tag{5}$$

where V is the velocity of the ice. For the 5mm ice $l_c$ = 30mm, while for the 25mm ice $l_c$ = 100mm. The maximum in surge force occurs at V = 0.05m/s for the 5 mm thick ice, and at V = 0.20m/s for the 25-millimeter-thick ice. Thus the critical values of t in these two cases are t = 0.6s for the 5mm thick ice and t = 0.5s for the 25-millimeter-thick ice. While there is considerable scatter affecting this analysis both in terms of the position of the maximum and the distribution of ice sizes, it is interesting to note that both values of $t_{crit}$ are approximately 1/8th of the natural period of the surge force, or the third harmonic of the resonant frequency. Thus the maxima observed may be a resonance effect. Supporting this is the fact that no maximum is apparent for the 5-millimeter-thick ice in the 100-millimeter-layer tests. In this case, many pieces of ice would be impacting the platform almost continually, in contrast to the single layer tests in which a resonance effect should be readily apparent.

## V. CONCLUSIONS

While this work was intended as a preliminary investigation of loads on moored platforms due to ice rubble, the following conclusions can be made:

1. In contrast to the behavior observed by Matsuishi and Ettema (1985a), some degree of cyclic behavior was observed in the surge force. This arose because, rather than a stable ice prow forming at the leading edge of the platform, a prow would form and then slough off to the side at which point the platform would move forward rapidly. As another prow formed the platform was again pushed back until the new prow sloughed off.

2. Mean and peak values of heave and surge force increased monotonically with the thickness of the rubble layer. Peak values of pitch also increased monotonically with layer thickness, although the mean value of pitch angle decreased for the thickest rubble layer.

3. For those tests in which the platform was stationary (i.e., connected to the instrument beam), both heave and surge force peak values exhibited an apparent maximum with respect to velocity of rubble layer. This may arise from resonance effects, though more experimental data are needed to clarify this point.

4. Although scattered, the peak values of pitch appeared constant with ice velocity.

5. Both heave and surge forces were greater for the towed platform than for the stationary platform. This is thought to arise from boundary effects.

Table 1

Principal Dimensions of the Test Platform and "Kulluk"

| | Test Platform (1/45 scale) | "Kulluk" |
|---|---|---|
| Diameter at deck level (m) | 1.8 | 81.0 |
| Diameter at load waterline (m) | 1.5 | 67.5 |
| Diameter at base line (m) | 1.334 | 60.0 |
| Depth (m) | 0.334 | 15.5 |
| Draft (m) | 0.187 | 8.4 |
| Displacement ($m^3$) | 0.271 | 24700 |
| Cone Angle (degree) | 31.4 | 31.4 |

Table 2

Calibration Coefficients for Test Transducer

| Transducer | Coefficient |
|---|---|
| Load Cell | 17.62 N/Volt |
| LVDT #1 | 12.7 mm/Volt |
| LVDT #2 | 12.7 mm/Volt |

Table 3

Rubble Size Distributions and Layer Porosities

| 5mm Thick Ice Sizes (mm) | Count | 25mm Thick Ice Sizes (mm) | Count |
|---|---|---|---|
| 90-80 | 3 | 200-240 | 1 |
| 70-75 | 5 | 130-150 | 3 |
| 35-65 | 10 | 60-80 | 4 |
| 25-30 | 10 | 40-60 | 5 |
| <25 | 0.1 liter | 30-30 | 21 |
| | | <30 | 0.5 liter |
| mean size $\bar{x}$ = 49.5mm | a = 65.3mm | mean size $\bar{x}$ = 57.0m | a = 53.8mm |

| Porosities | Sample Vol. ($mm^3$) | Mass (kg) | Porosity |
|---|---|---|---|
| 5mm Thick Ice | $3.35 \times 10^6$ | 1.66 | 35.9% |
| 25mm Thick Ice | $2.32 \times 10^6$ | 1.35 | 36.7% |

Table 4

Platform attached to Instrument Beam

| Test. No. | Ice Thickness (mm) | Layer Thickness (mm) | Velocity (m/s) | $\bar{F}$ (N) | 2σ | H (mm) | 2σ | $\bar{P}$ (degrees) | 2σ |
|---|---|---|---|---|---|---|---|---|---|
| R102 | 5 | 5 | .02 | 5.11 | 3.44 | -.145 | 0.146 | -.049 | 0-.030 |
| R104 | 5 | 5 | .04 | 6.73 | 1.73 | -.148 | 0.080 | -.049 | 0.006 |
| R110 | 5 | 5 | .10 | 6.91 | 4.76 | -.177 | 0.086 | -.050 | 0.018 |
| R120 | 5 | 5 | .20 | 3.17 | 0.91 | -.061 | 0.156 | -.039 | 0.010 |
| R202 | 5 | 50 | .02 | 20.8 | 11.8 | -.420 | 0.428 | -.067 | 0.046 |
| R204 | 5 | 50 | .04 | 32.3 | 22.3 | -.521 | 0.976 | -.050 | 0.114 |
| R210 | 5 | 50 | .10 | 24.4 | 10.4 | -.604 | 0.342 | -.073 | 0.028 |
| R220 | 5 | 50 | .20 | 25.1 | 17.5 | -.709 | 0.964 | -.132 | 0.098 |
| R204A | 5 | 50 | .04 | 44.3 | 30.3 | -1.10 | 1.218 | -.087 | 0.106 |
| R302 | 5 | 100 | .02 | 59.9 | 28.9 | -1.77 | 1.450 | -.064 | 0.108 |
| R304 | 5 | 100 | .04 | 56.3 | 34.6 | -1.51 | 1.098 | -.082 | 0.136 |
| R310 | 5 | 100 | .10 | 77.8 | 14.4 | -2.27 | 1.222 | -.071 | 0.146 |
| R320 | 5 | 100 | .20 | 63.0 | 25.8 | -1.69 | 0.722 | -.065 | 0.092 |
| R304A | 5 | 100 | .04 | 57.5 | 31.7 | -1.50 | 1.258 | -.083 | 0.124 |
| T102 | 25 | 25 | .02 | 33.3 | 24.5 | -.759 | 0.586 | -.060 | 0.060 |
| T104 | 25 | 25 | .04 | 34.4 | 11.6 | -.702 | 0.192 | -.063 | 0.066 |
| T110 | 25 | 25 | .10 | 37.5 | 15.2 | -.769 | 0.680 | -.092 | 0.090 |
| T120 | 25 | 25 | .20 | 48.2 | 38.0 | -.954 | 0.942 | -.072 | 0.134 |
| T102A | 25 | 25 | .02 | 30.0 | 20.9 | -.646 | 0.572 | -.074 | 0.054 |

## Table 5

### Platform Towed by Carriage

| Test No. | Ice Thickness (mm) | Layer Thickness (mm) | Velocity (m/s) | $\bar{F}$ (N) | 20 | $\bar{H}$ (mm) | 20 | $\bar{P}$ (degrees) | 20 |
|---|---|---|---|---|---|---|---|---|---|
| TW102 | 5 | 5 | .02 | 19.5 | 4.75 | -.126 | 0.282 | -.035 | 0.030 |
| TW104 | 5 | 5 | .04 | 12.6 | 2.99 | -0.95 | 0.394 | -.048 | 0.026 |
| TW110 | 5 | 5 | .10 | 14.7 | 2.97 | -1.11 | 0.210 | -.054 | 0.020 |
| TW120 | 5 | 5 | .20 | 18.2 | 13.2 | -0.97 | 0.508 | -.080 | 0.039 |
| TW104A | 5 | 5 | .04 | 19.7 | 3.14 | -1.41 | 0.264 | -.064 | 0.032 |
| TW202 | 5 | 50 | .02 | 47.9 | 10.8 | -2.25 | 0.792 | -.106 | 0.054 |
| TW204 | 5 | 50 | .04 | 55.2 | 11.7 | -3.19 | 0.720 | -.081 | 0.058 |
| TW210 | 5 | 50 | .10 | 41.5 | 15.9 | -2.24 | 1.010 | -.100 | 0.0709 |
| TW220 | 5 | 50 | .20 | 43.7 | 20.8 | -2.53 | 0.976 | -.146 | 0.062 |
| TW204A | 5 | 50 | .04 | 45.2 | 6.07 | -2.07 | 0.704 | -.048 | 0.034 |
| TW320 | 5 | 100 | .20 | 64.0 | 21.7 | -4.21 | 1.38 | -.070 | 0.156 |
| TW310 | 5 | 100 | .10 | 71.7 | 18.8 | -3.97 | 1.18 | -.065 | 0.184 |
| TW304 | 5 | 100 | .04 | 76.0 | 14.1 | -4.29 | 1.67 | -.039 | 0.100 |

Table 6

Natural Periods and Logarithmic Decrements of the Model Platform

| | Surge | Heave | Pitch |
|---|---|---|---|
| Natural Period, T (seconds) | 4.50 | 1.41 | 1.17 |
| Natural Period in Ice | -- | 1.63 | 1.45 |
| Logarithmic decrement, $\delta$ | 0.25 | -- | 0.55 |

## REFERENCES


Ettema, R., Stern, F., and Lazaro, J. (1985), "Dynamics of Continuous-Mode Icebreaking by a Polar-Class Icebreaker Hull," IIHR Report No. 314.

Frederking, R. (1980), "Dynamic Ice Forces on an Inclined Structure", Physics and Mechanics of Ice, P. Tryde (Ed.), IUTAM Symposium, Copenhagen, Denmark.

Frederking, R. and Schwarz, J. (1982), "Model Test of Ice Forces on Fixed and Oscillating Cones", Cold Regions Science and Technology, Vol. 6, p. 61-72.

Greisman, P. (1981), "Brash Ice Behavior," Report No. CGRDC-9/81, U.S. Coast Guard Research and Development Center, Groton, CT.

Helleman, J.H. (1984), "Basic Investigations on Mush Ice," IAHR Ice Symposium, Vol. 3, pp. 37-55, Hamburg.

Hnatiuk, J. and Wright, B.D. (1984), "Ice Management to Support the Kulluk Drilling Vessel", Proc. 35th Annual Technical Meeting of Petroleum Society of CIM, Calgary, paper no. 84-96, p. 33-365.

Loh, J.K.S. and Stamberg, J.C. (1984), "New Generation Arctic Drilling System: Overview of First Year's Performance", Proc. 16th Offshore Technology Conference, Houston, paper no. 4797.

Matsuishi, M., and Ettema, R. (1985a), "Ice Loads and Motions Experienced by a Floating, Moored Platform in Mushy Ice Rubble", IIHR Report No. 295, The University of Iowa, Iowa City, Iowa.

Matsuishi, M. and Ettema, R. (1985b), "The Dynamic Behavior of a Floating, Cable-Moored Platform Continuously Impacted by Ice Floes", IIHR Report No. 294, The University of Iowa, Iowa City, Iowa.

Mellor, M. (1980), "Ship Resistance in Thick Brash Ice," Cold Regions Science and Technology, Vol. 3, pp. 305-321.

Milano, V. (1980), "A Reanalysis of Ship Resistance When in Continuous Motion Through Solid Ice", Intermarited 80, Hamburg, p. 456-475.

Milano, V. (1982), "Correlation of Analytical Prediction of Ship Resistance in Ice with Model and Full Scale Test Results", Intermarited 82, Hamburg, p. 350-372.

Nixon, W.A. and Ettema, R. (1987), "Ice Sheet Impact with a Floating, Cable-Moored Platform", IIHR Report in preparation.

Ralston, T.D. (1980), "Plastic Limit Analysis of a Sheet Loads on Conical Structures", Physics and Mechanics of Ice, P. Tryde (Ed.), IUTAM Symposium, Copenhagen, p. 289-308.

Wessels, E. (1984), "Model Test Investigation of Ice Forces on Fixed and Floating Conical Structures", IAHR Ice Symposium, Vol. 3, p. 203-219, Hamburg

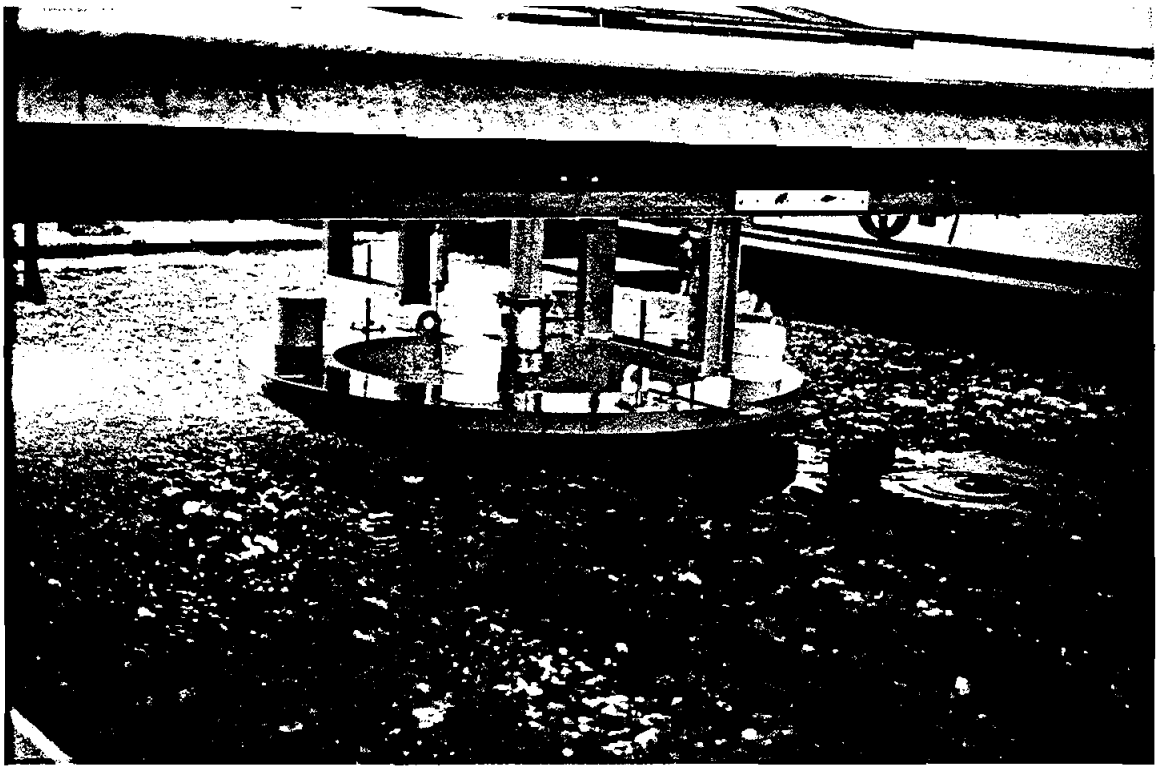

Figure 1. The test platform

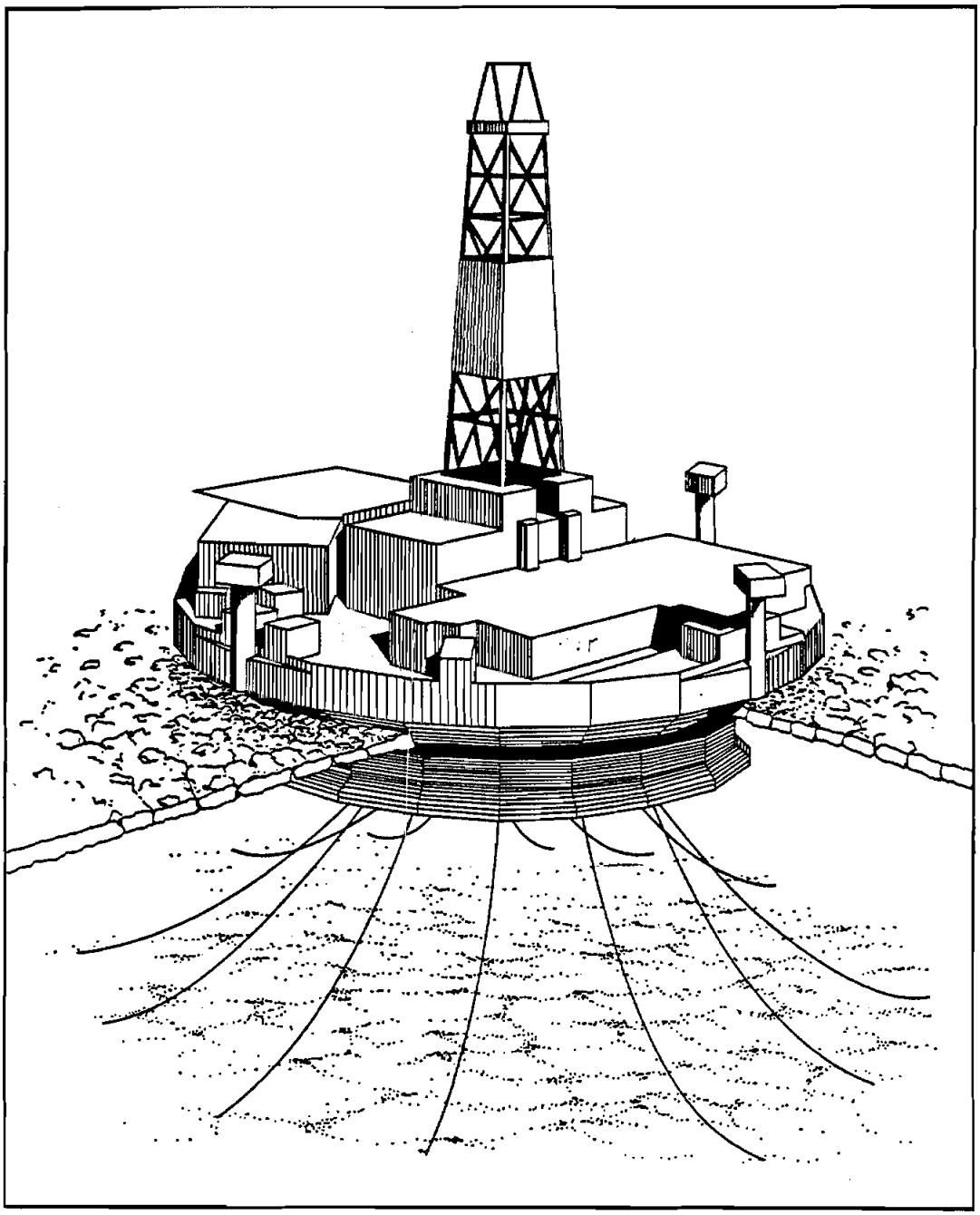

Figure 2. A floating, cable-moored platform of conical hull form

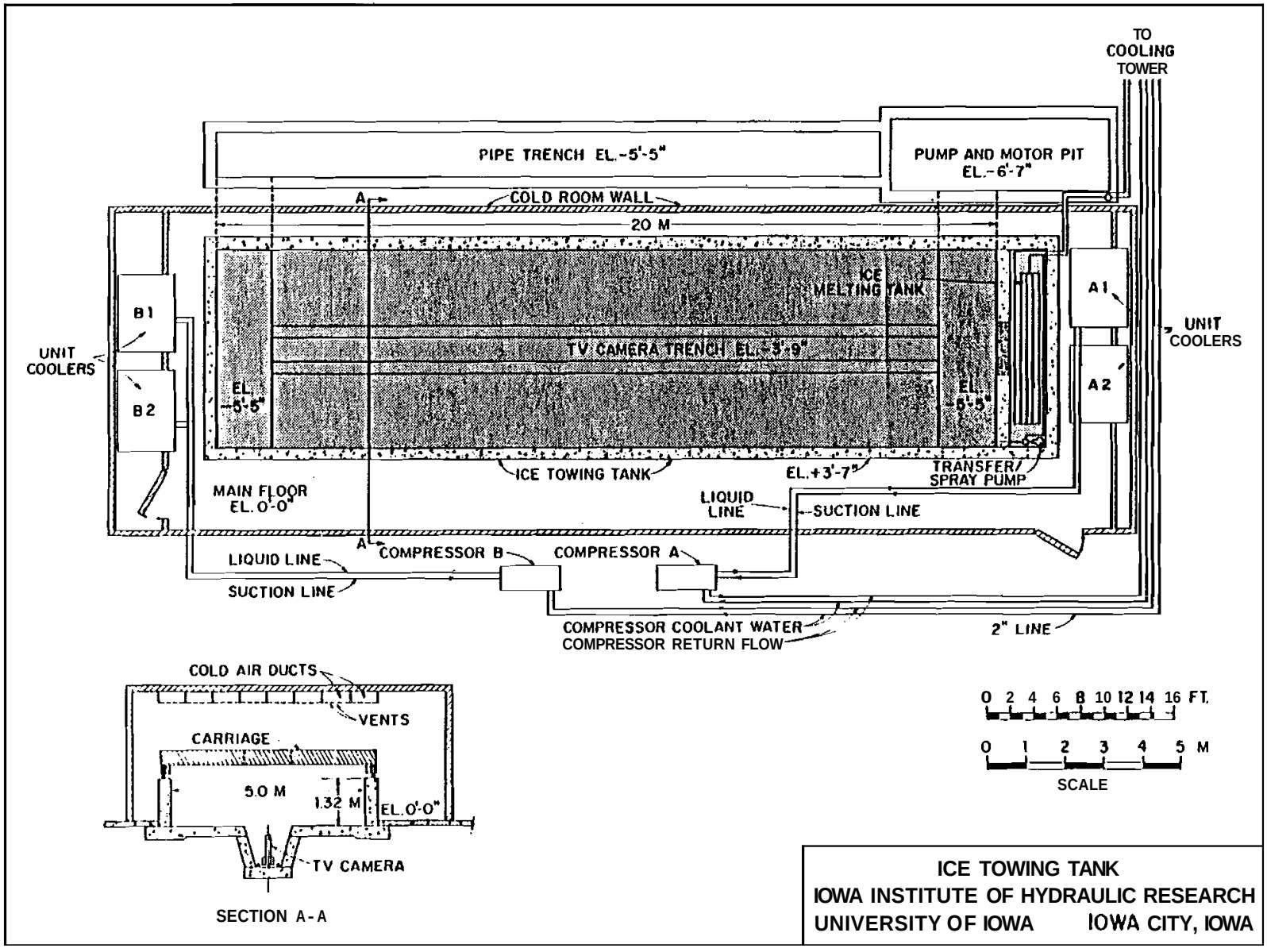


Figure 3. Ice towing tank

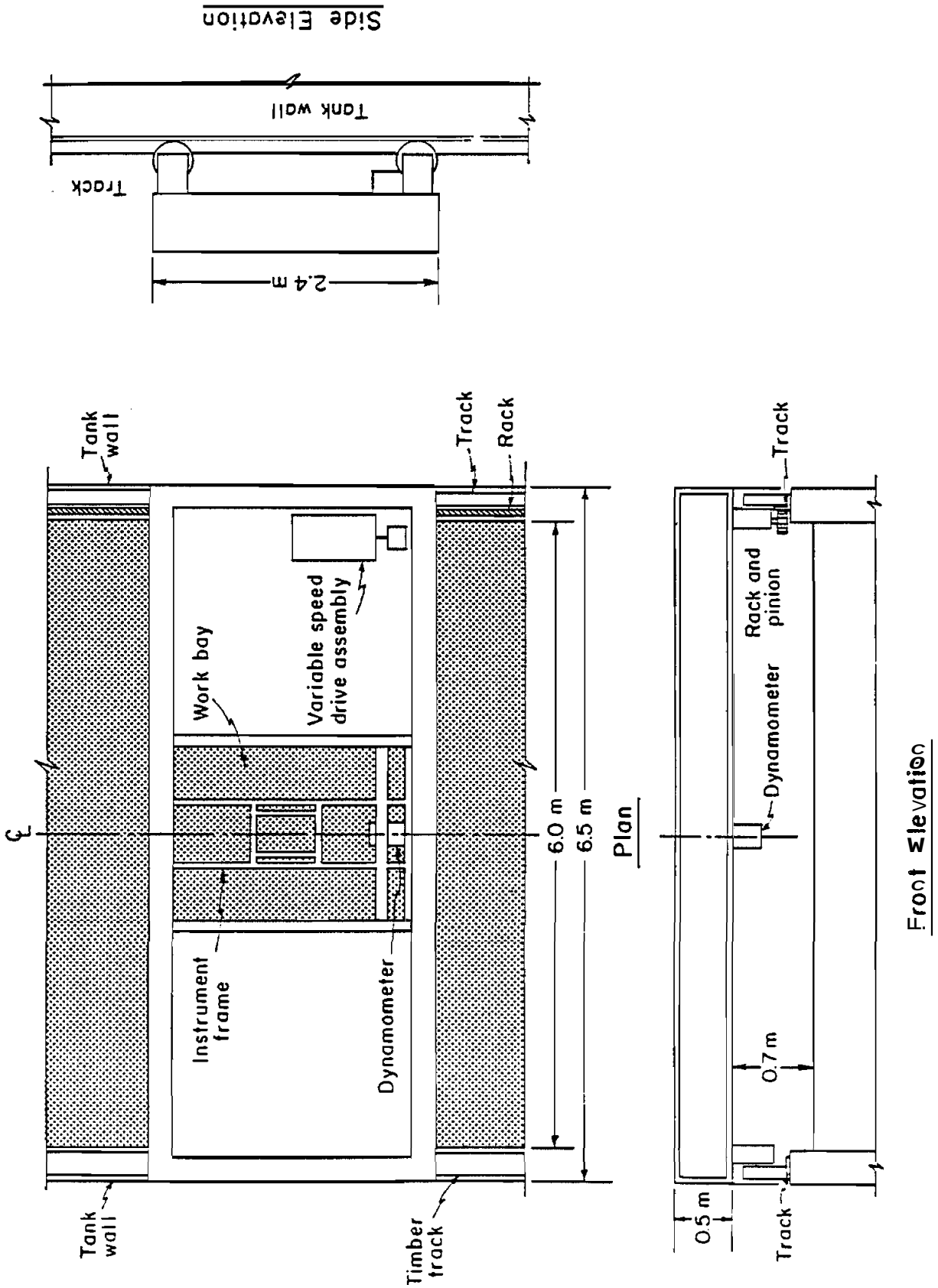


Figure 4. The towing carriage

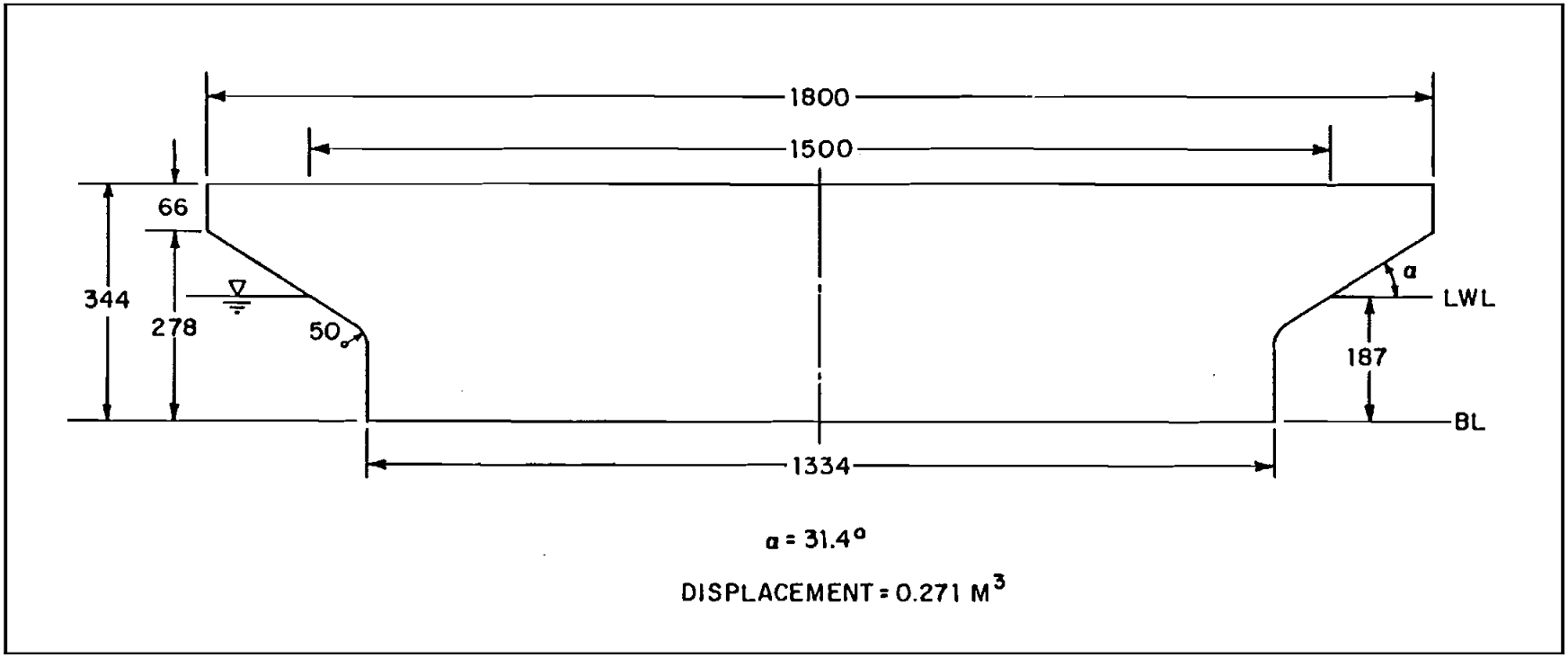


Figure 5. Geometry and dimensions of the test platform

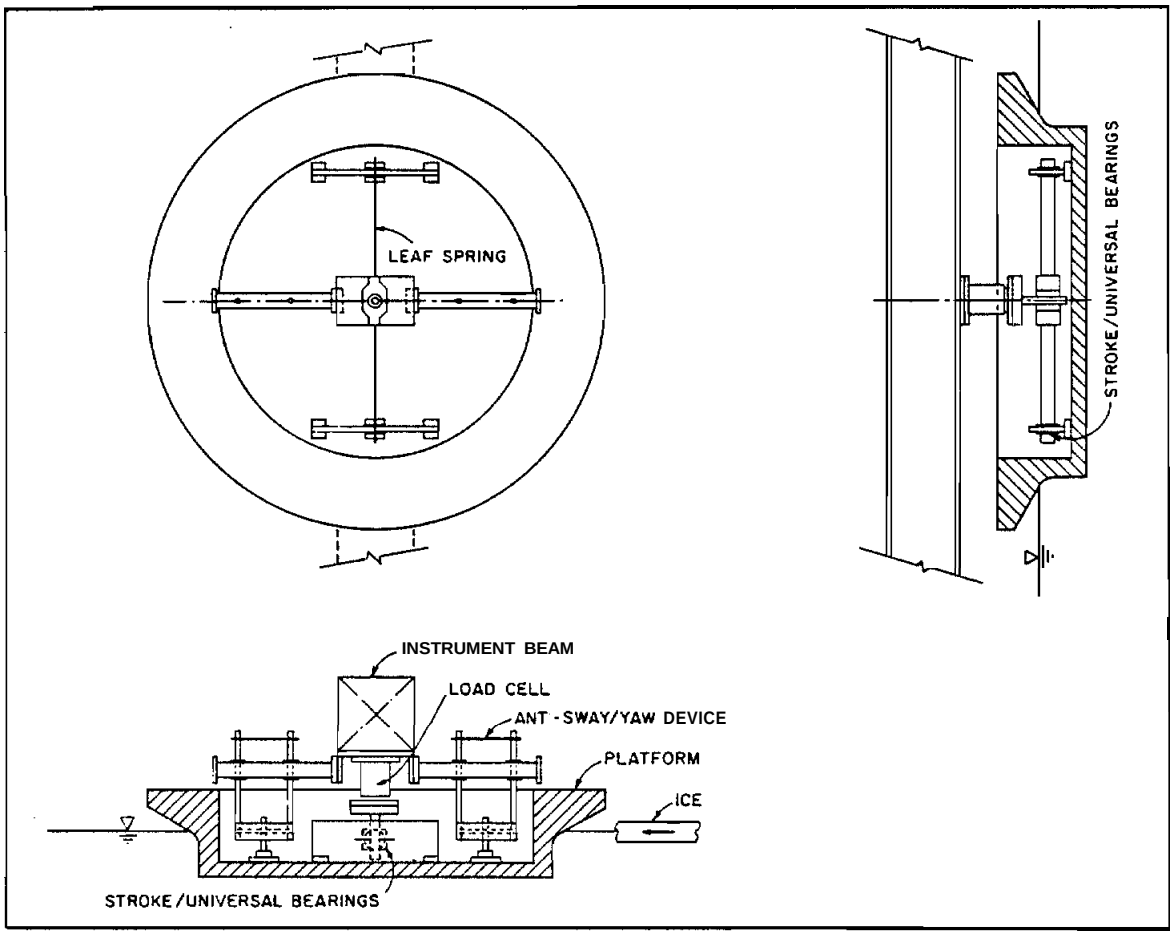


Figure 6. instrumentation of the test platform

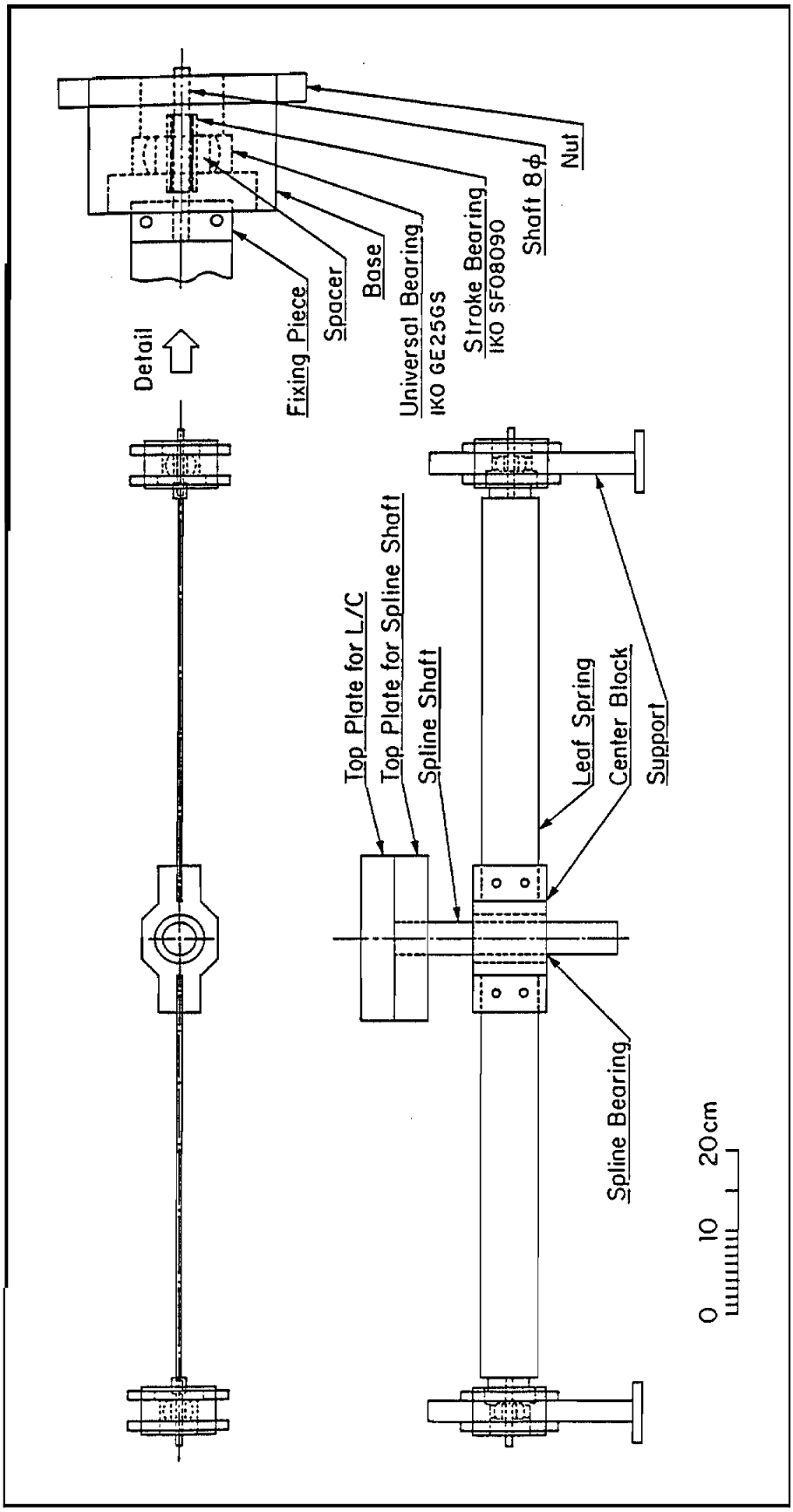


Figure 7. The mooring harness

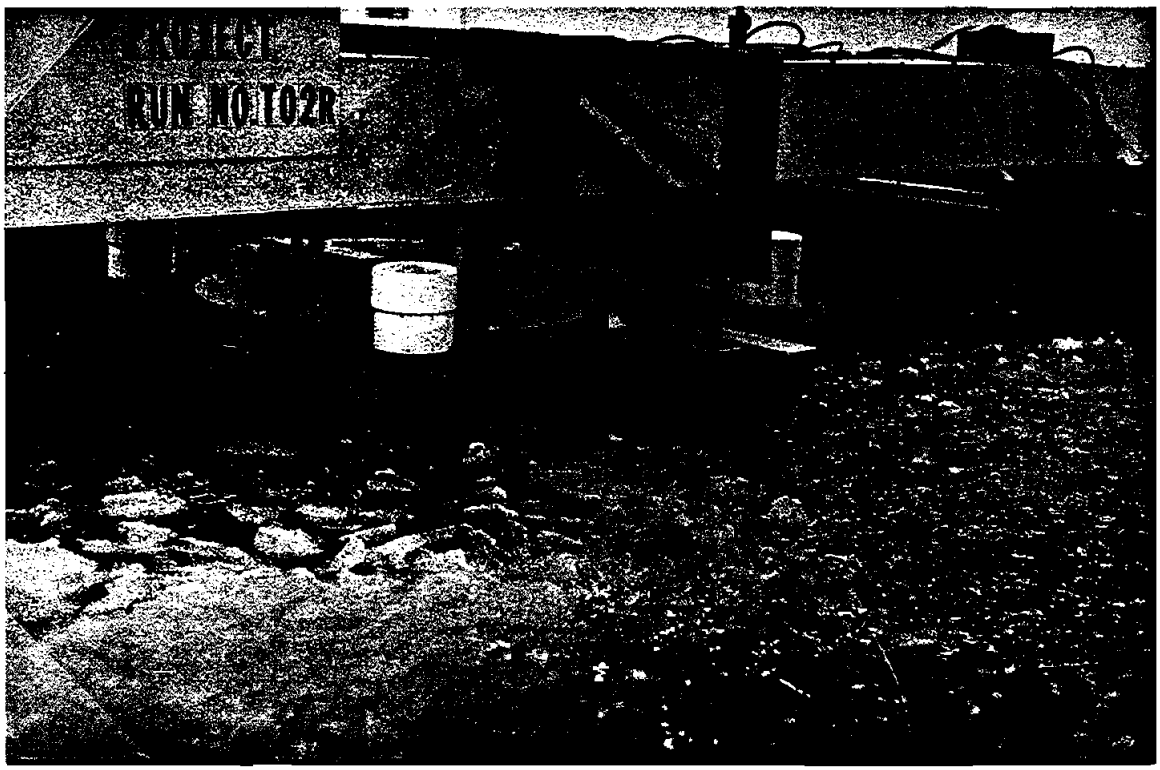

**Figure 8. The sway and yaw restraining devices**

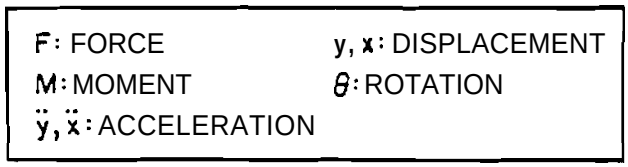


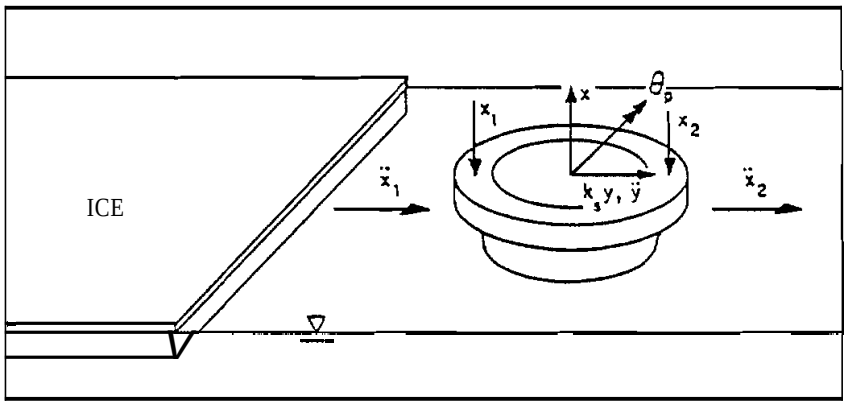


(a) MOORED PLATFORM

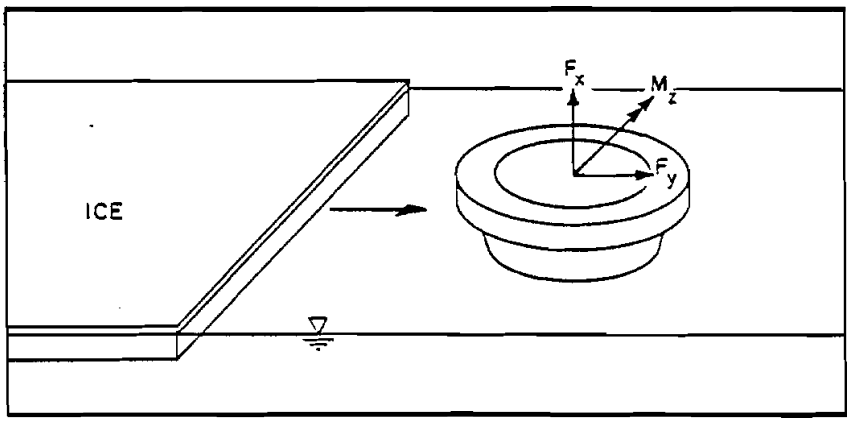


(b) FIXED PLATFORM

Figure 9. Locations of transducers and positive directions

(a) 5 mm thick rubble

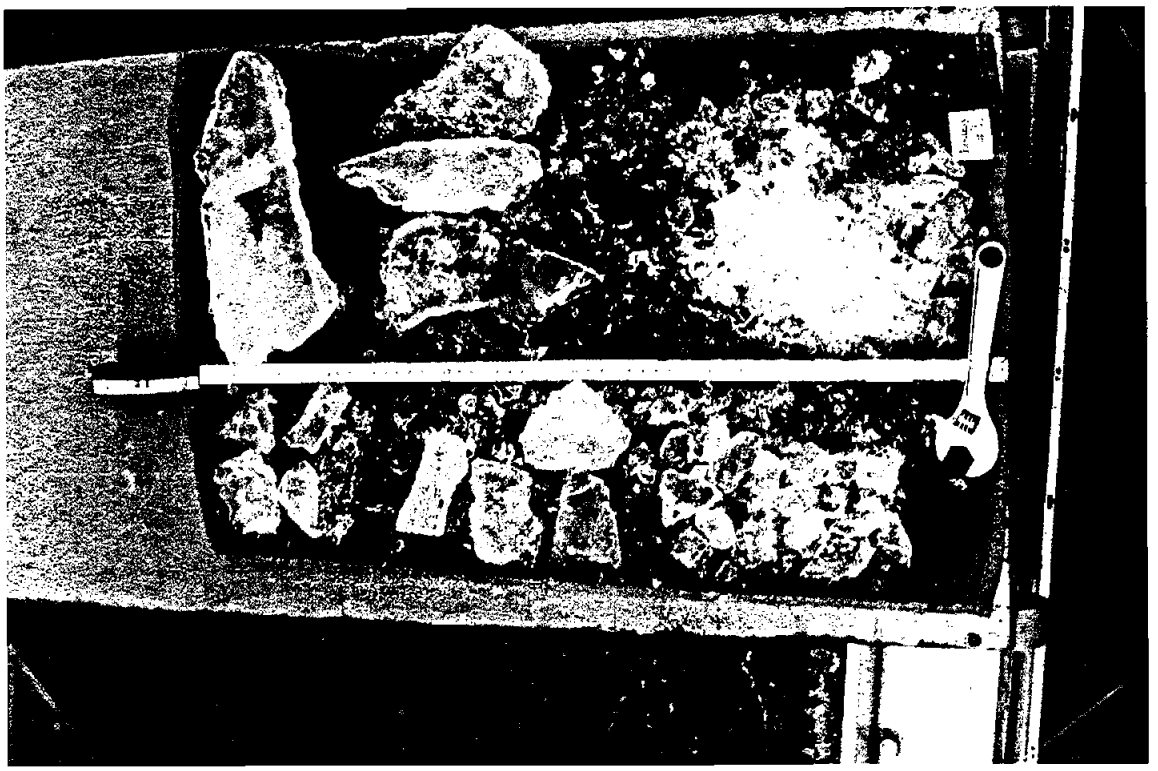

(b) 25 mm thick rubble

Figure 10. Comparison of 5 mm and 25 mm thick rubble

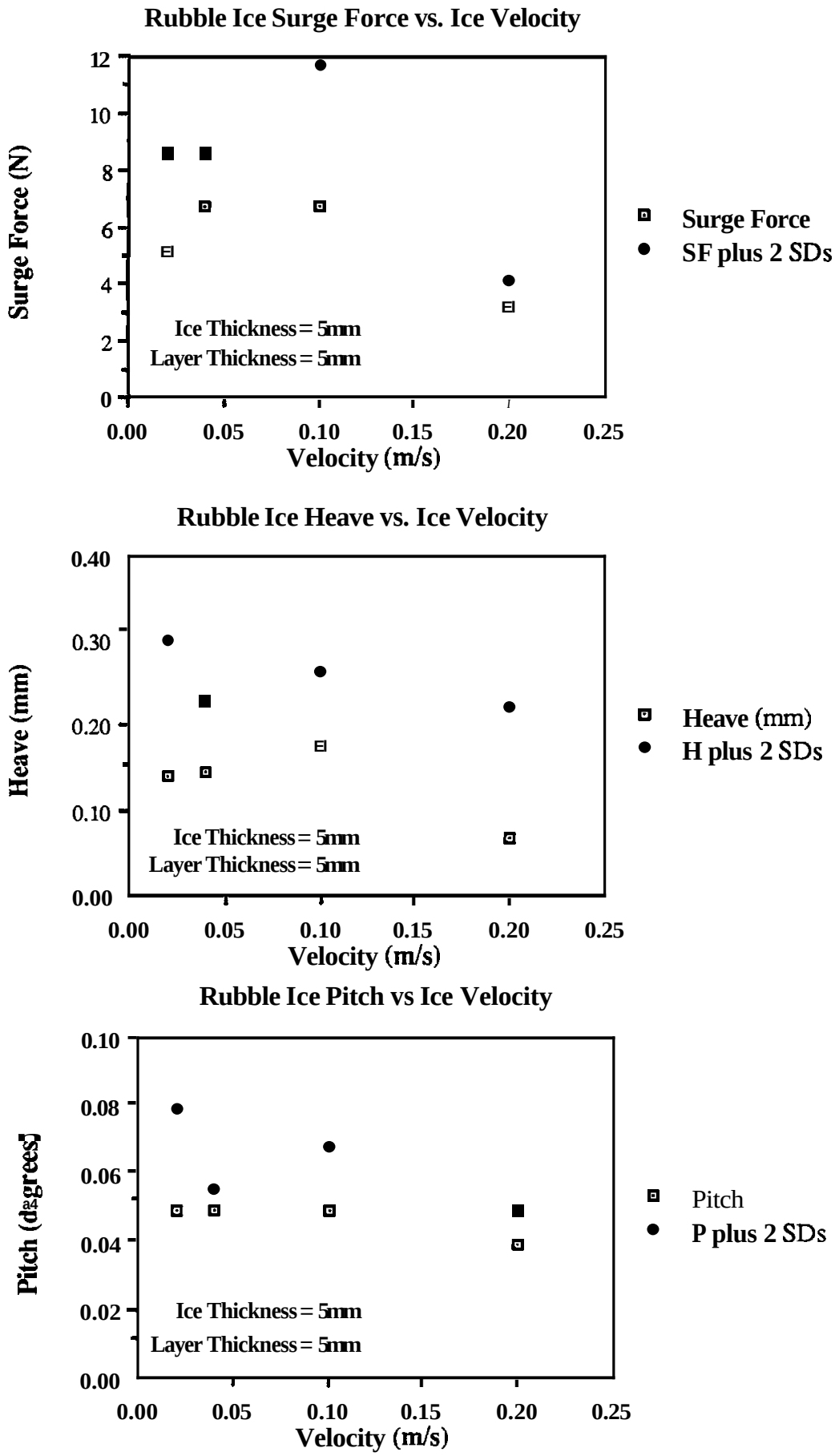


Figure 11. Heave, surge force and pitch vs ice velocity; ice thickness = 5 mm, layer thickness = 5 mm

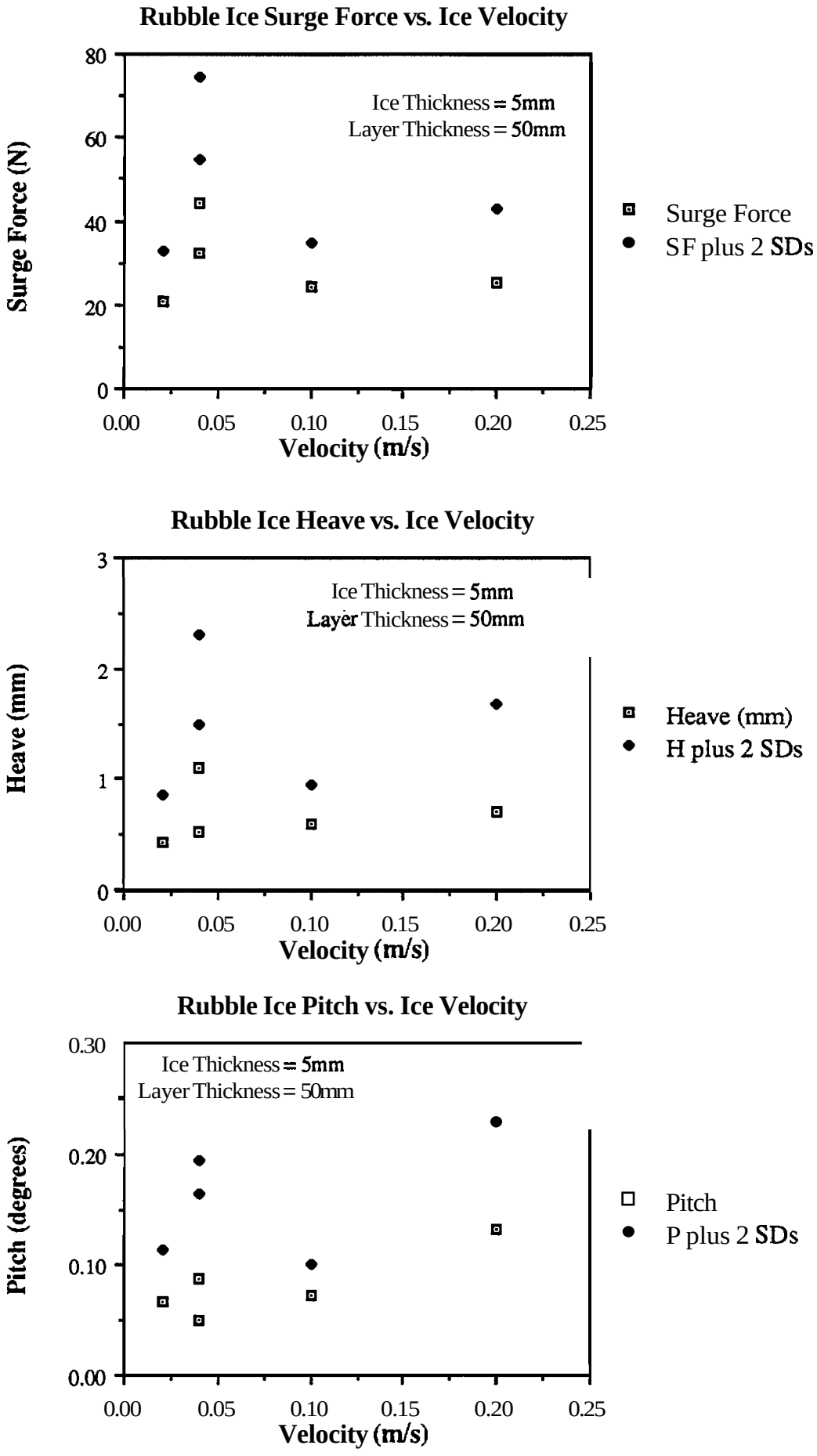


Figure 12. Heave, surge force and pitch vs ice velocity; ice thickness = 5 mm, layer thickness = 50 mm

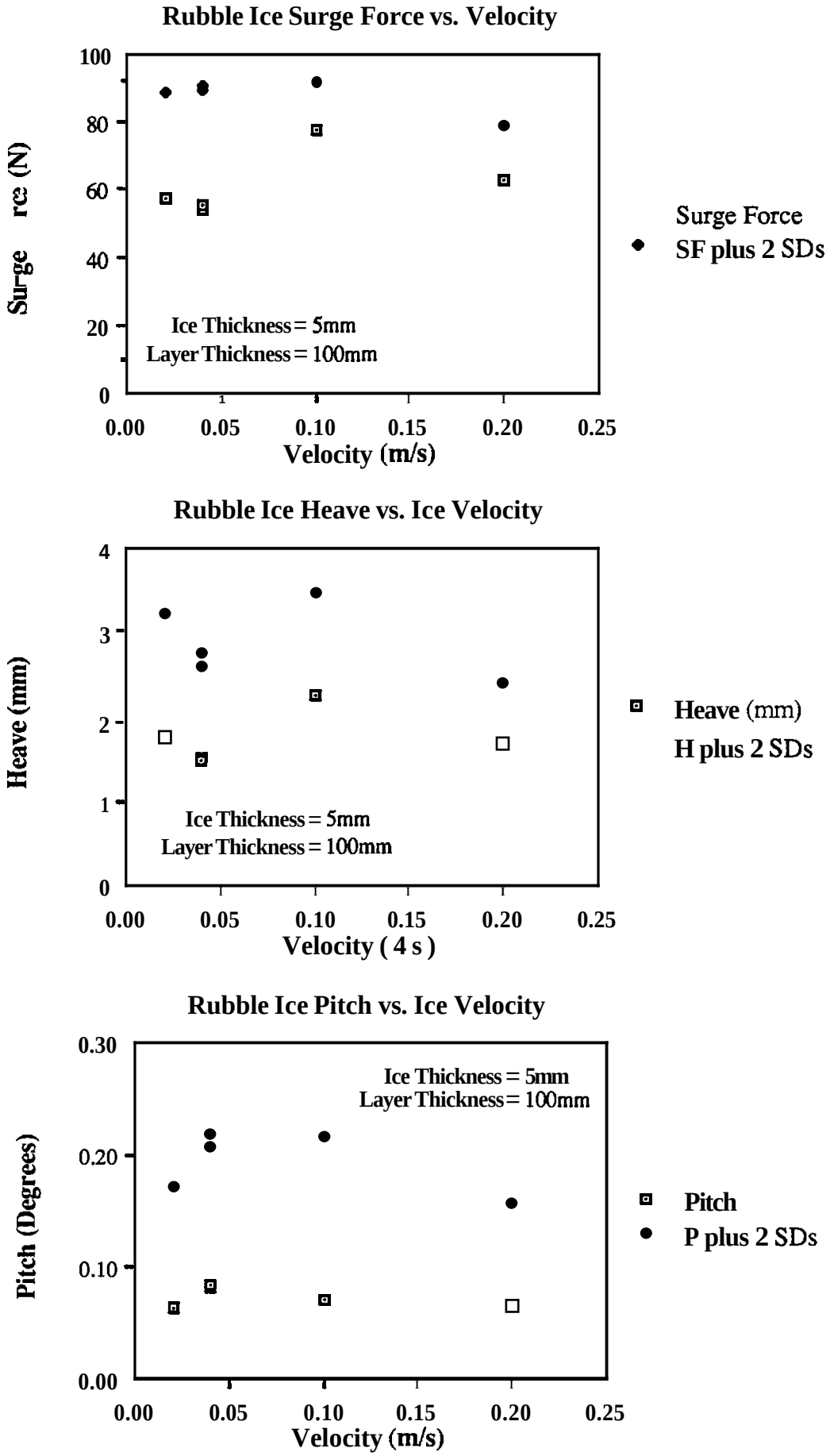


Figure 13. Heave, surge force and pitch vs ice velocity; ice thickness = 5 mm, layer thickness = 100 mm

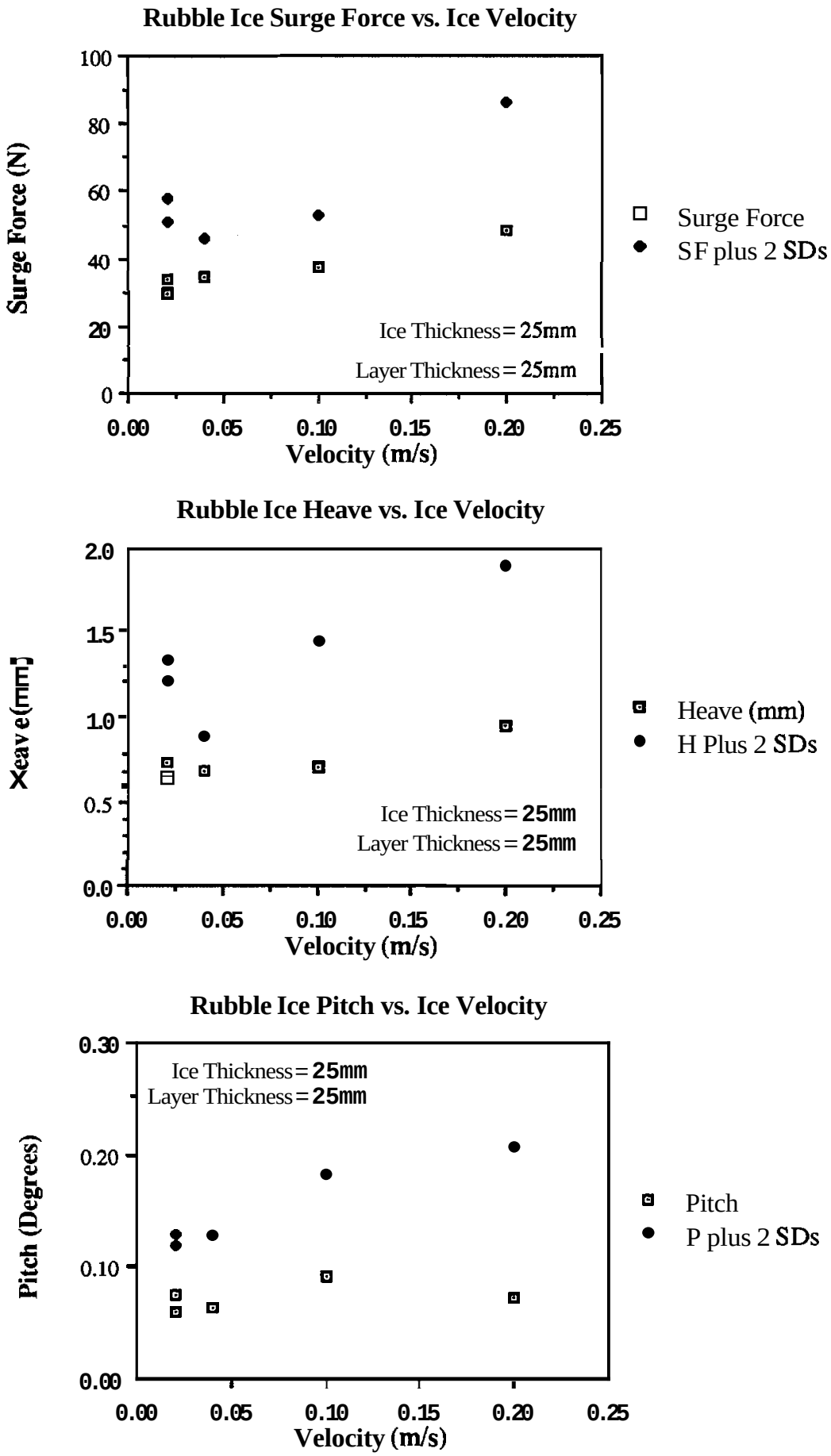


Figure 14. Heave, surge force and pitch vs ice velocity; ice thickness = 25 mm, layer thickness = 25 mm

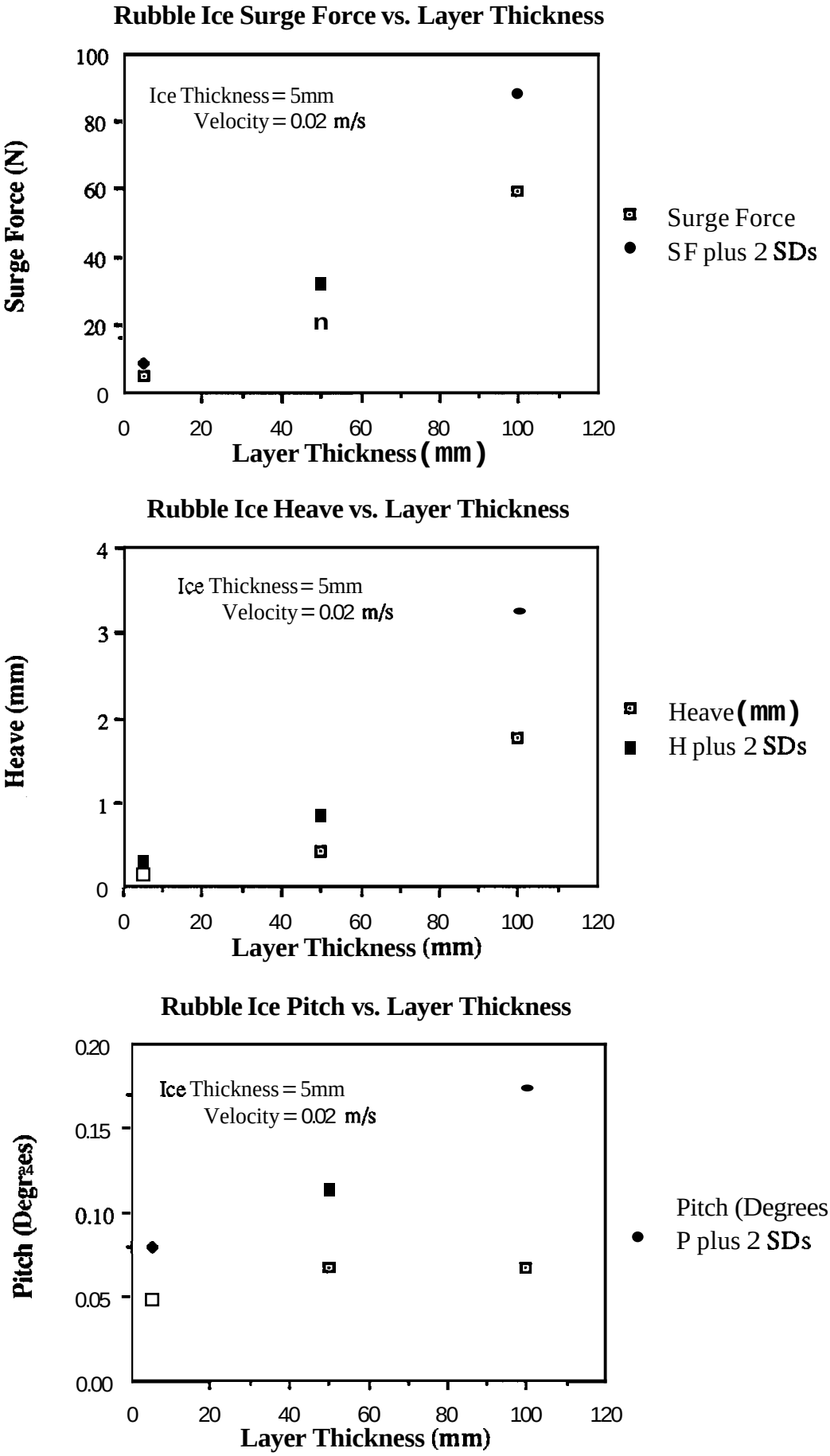


Figure 15. Heave, surge force and pitch vs layer thickness; ice thickness = 5 mm, velocity = 0.02 m/s

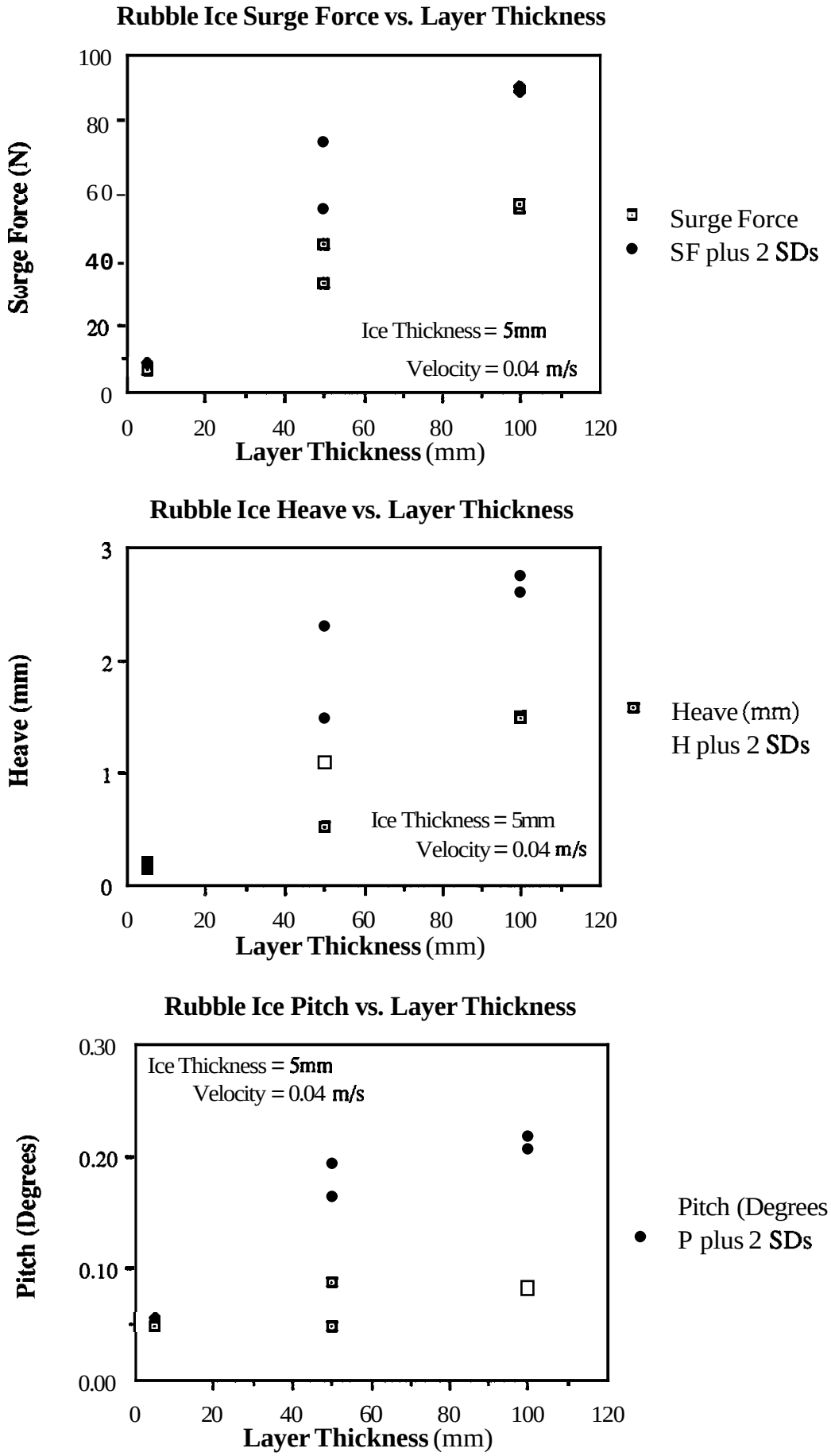


Figure 16. Heave, surge force and pitch vs layer thickness; ice thickness = 5 mm, velocity = 0.04 m/s

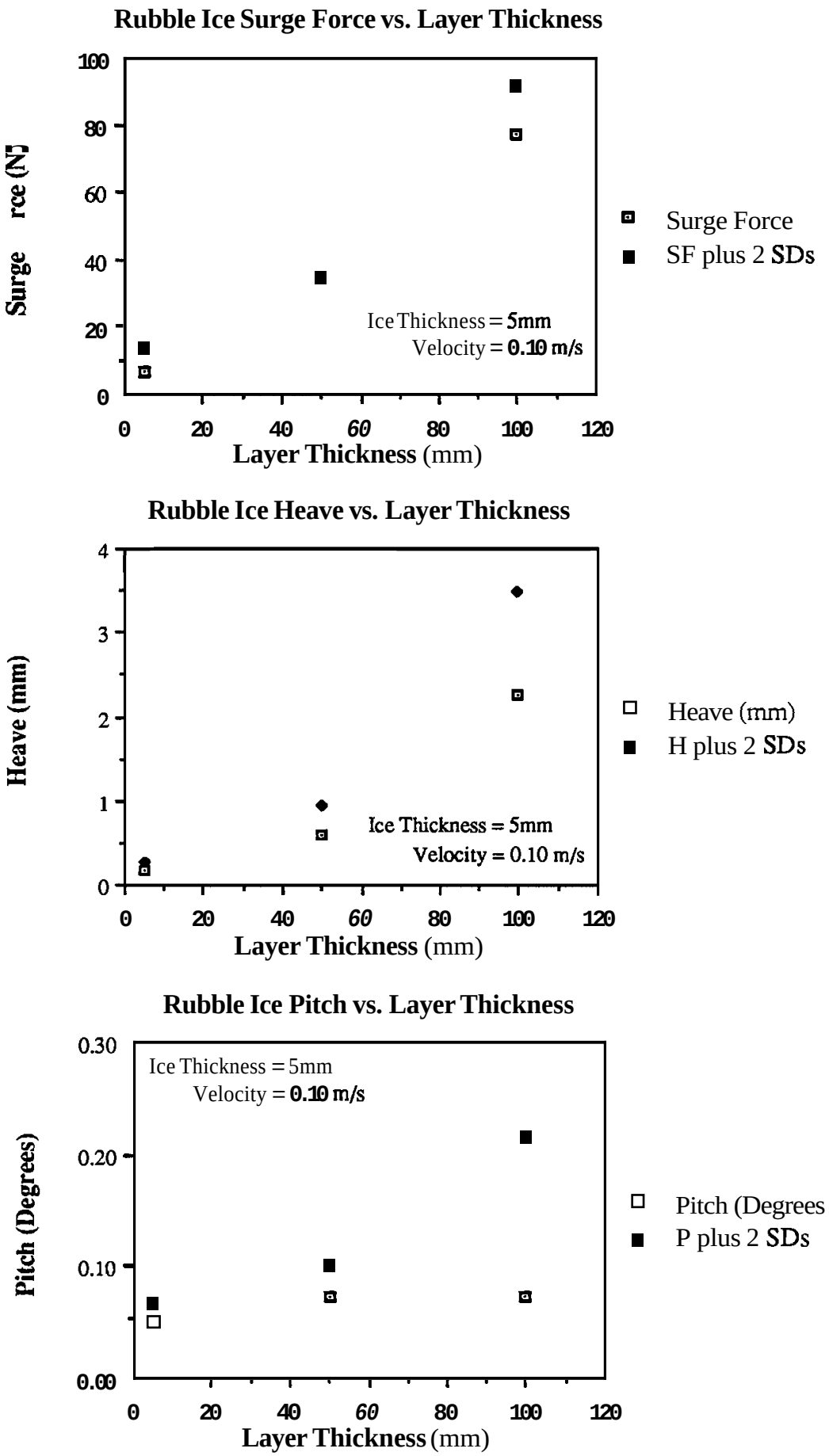


Figure 17. Heave, surge force and pitch vs layer thickness; ice thickness = 5 mm, velocity = 0.10 m/s

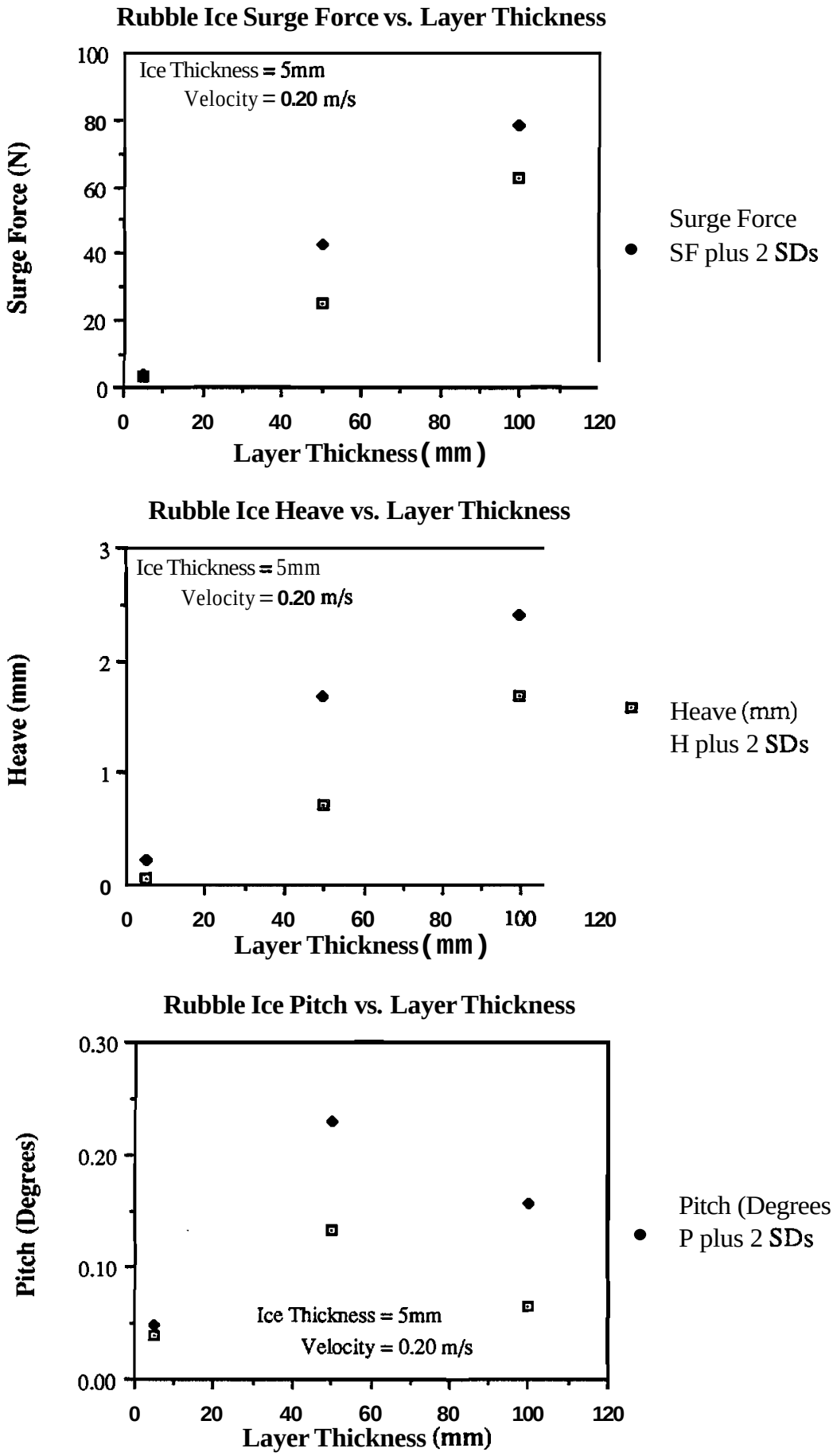


Figure 18. Heave, surge force and pitch vs layer thickness; ice thickness = 5 mm, velocity = 0.20 m/s

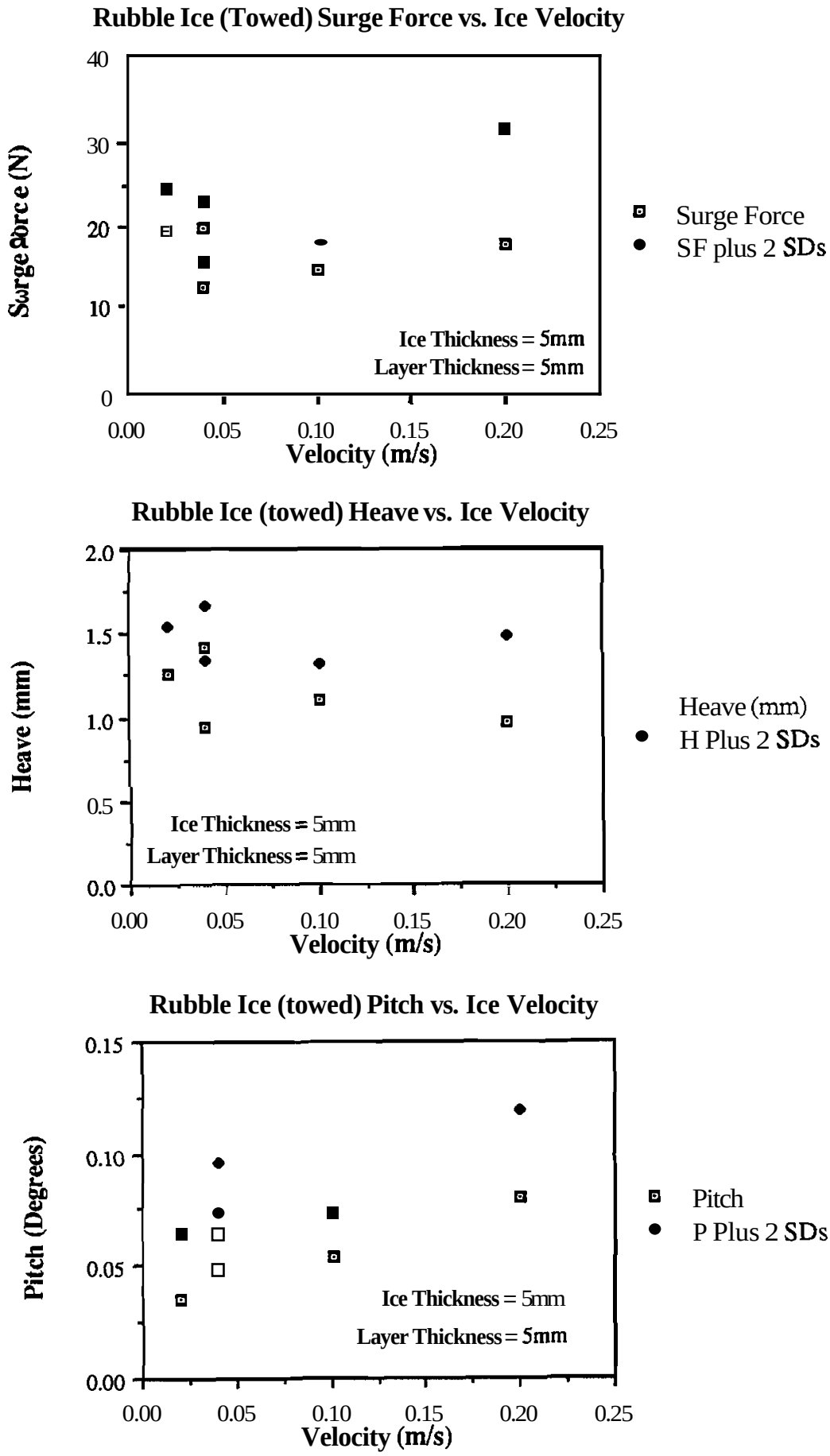


Figure 19, Heave, surge force and pitch vs ice velocity (towed platform); ice thickness = 5 mm, layer thickness = 5 mm

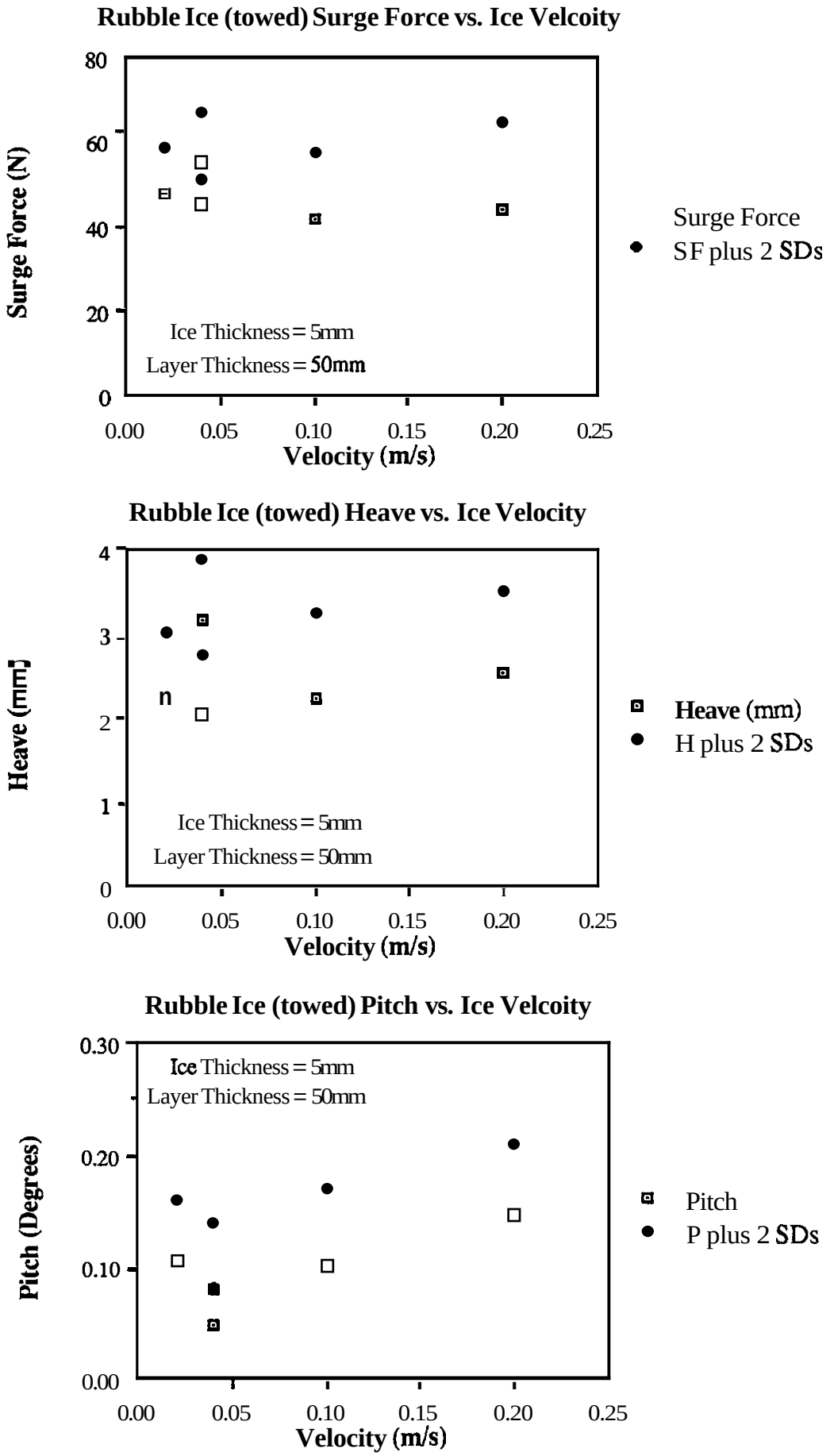


Figure 20. Heave, surge force and pitch vs ice velocity (towed platform); ice thickness = 5 mm, layer thickness = 50 mm

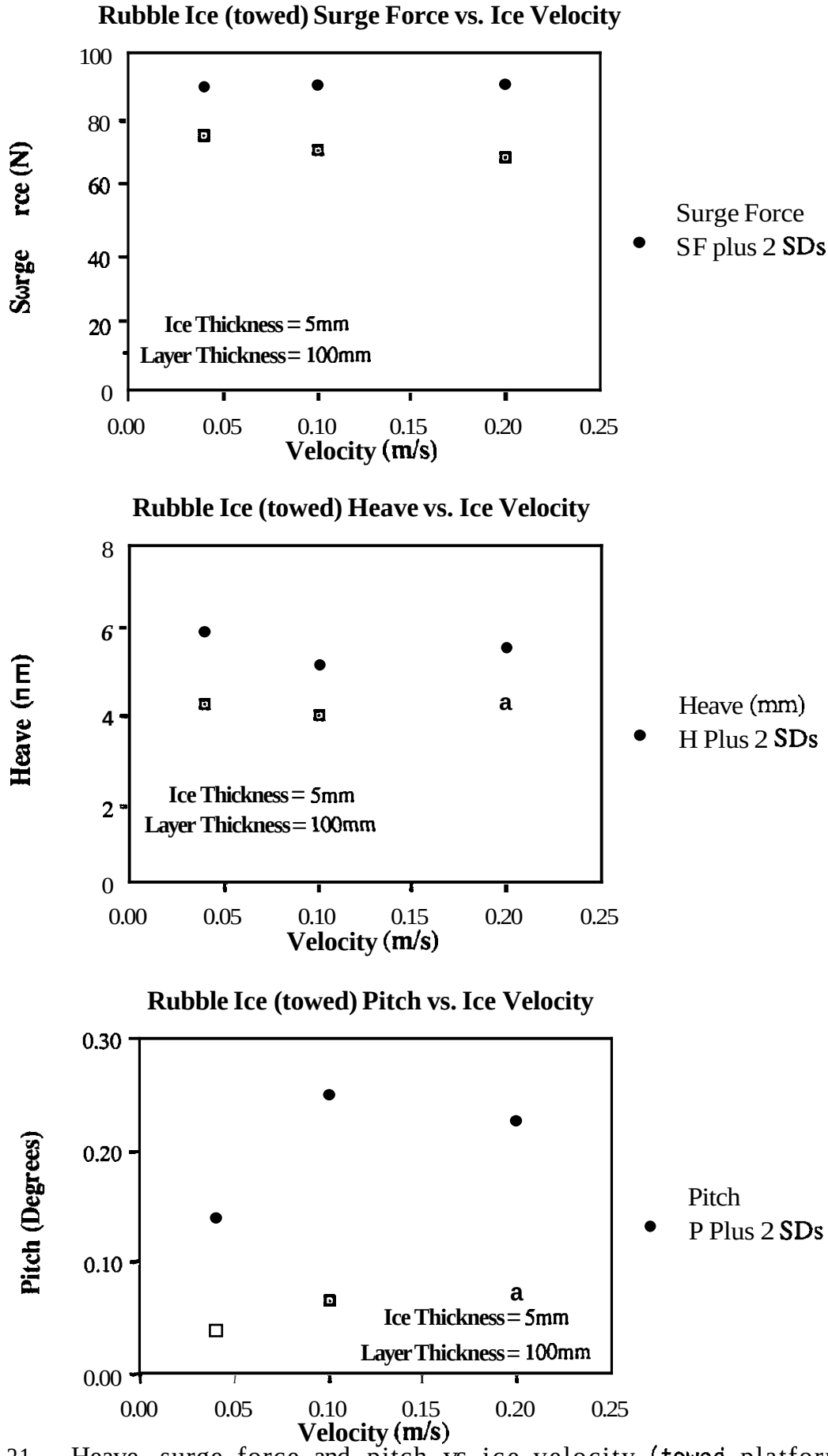


Figure 21. Heave, surge force and pitch vs ice velocity (towed platform); ice thickness = 5 mm, layer thickness = 100 mm

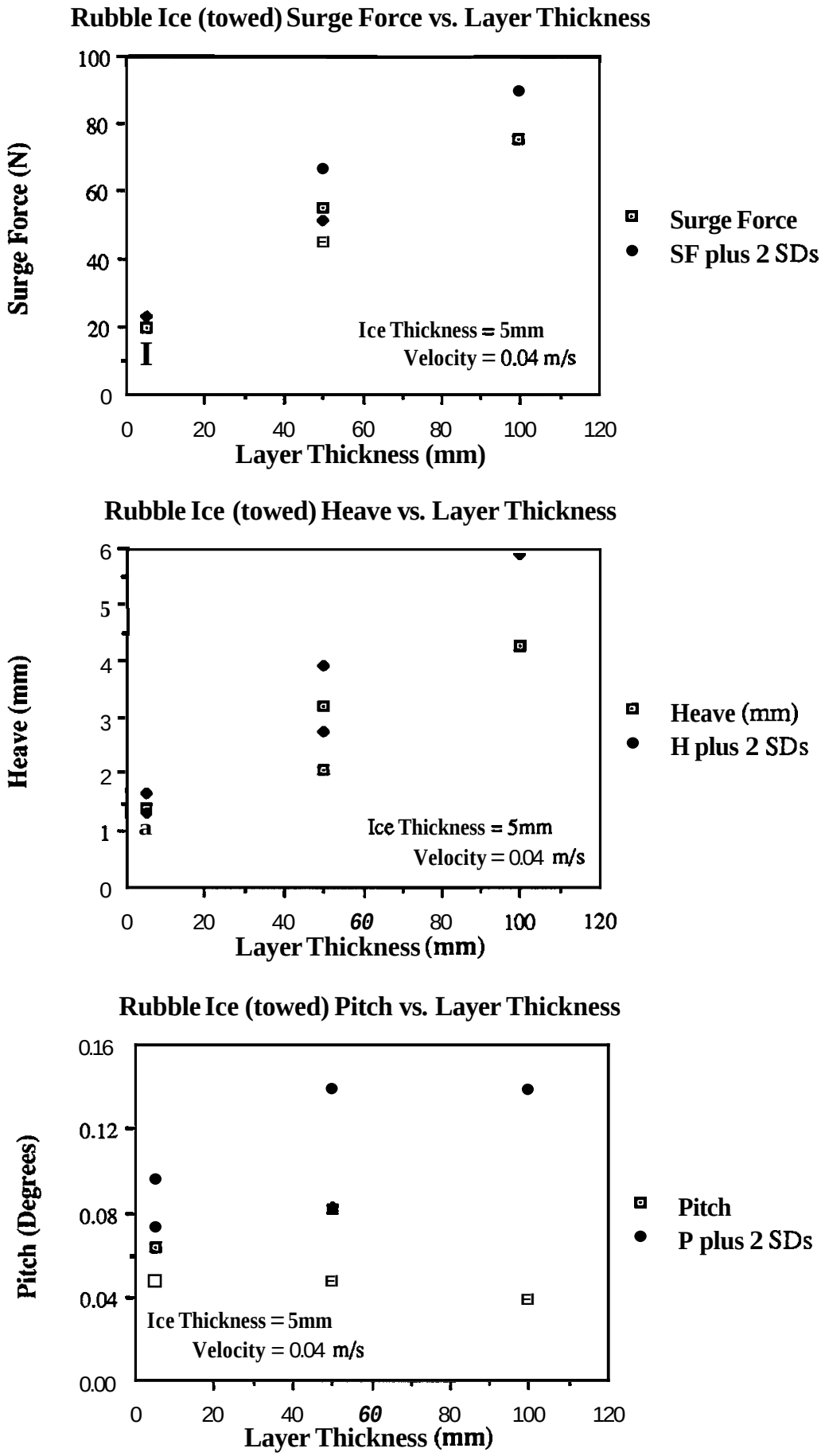


Figure 22. Heave, surge force and pitch vs layer thickness (towed platform); ice thickness = 5 mm, layer thickness = 0.04 m/s

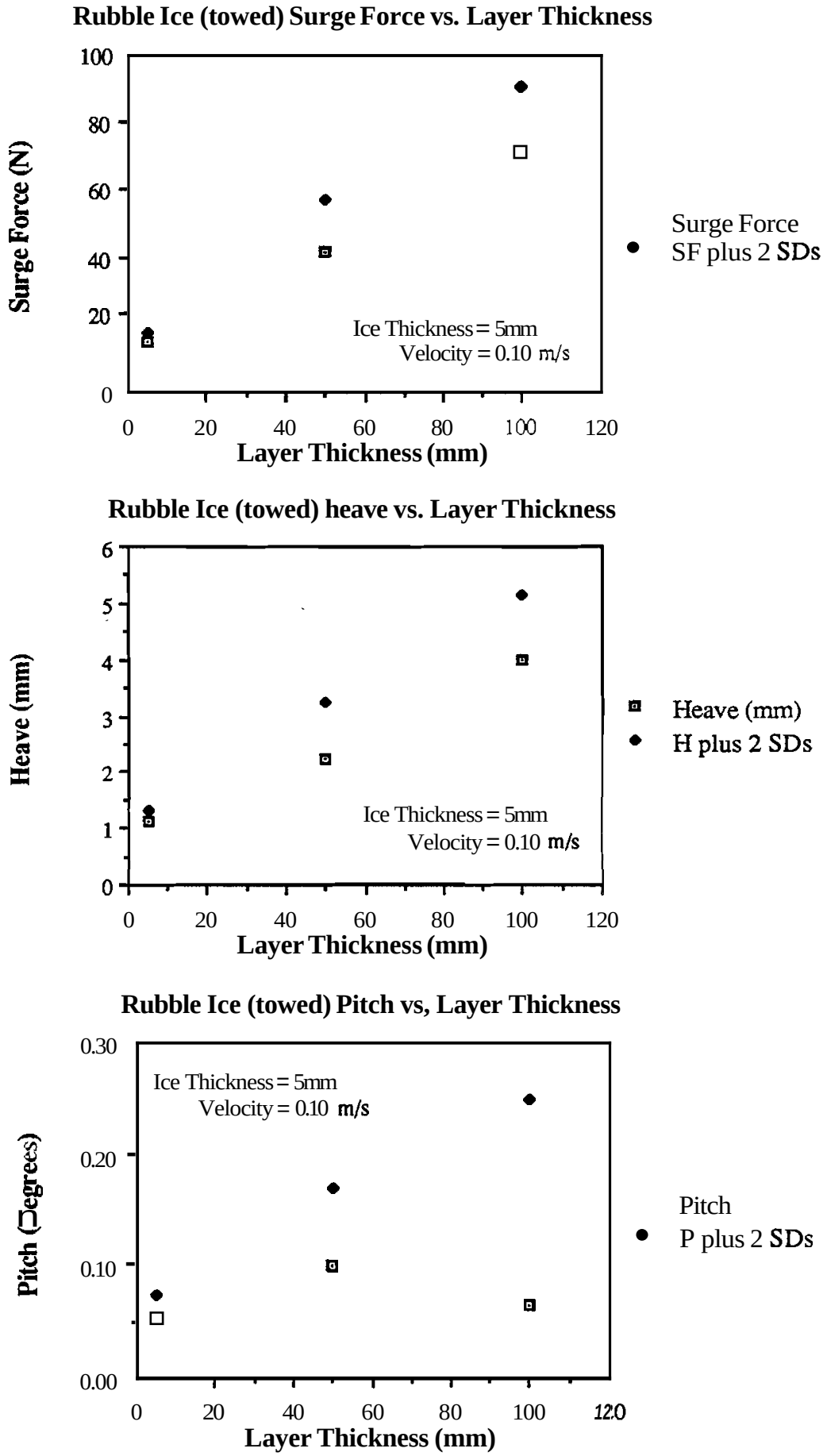


Figure 23. Heave, surge force and pitch vs layer thickness (towed platform); ice thickness = 5 mm, layer thickness = 0.10 m/s

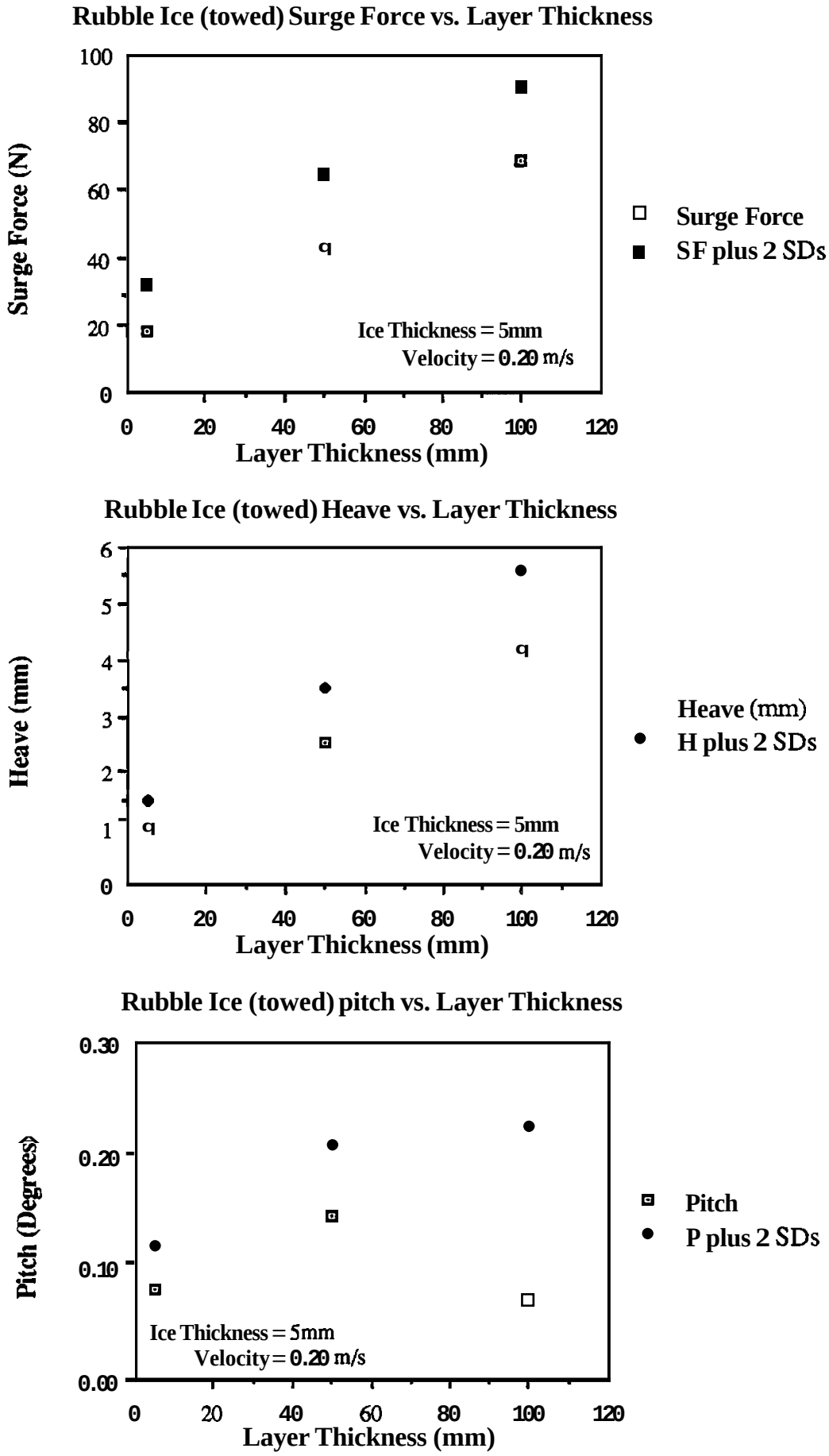


Figure 24. Heave, surge force and pitch vs iayer thickness (towed platform); ice thickness = 5 mm, layer thickness = 0.20 m/s

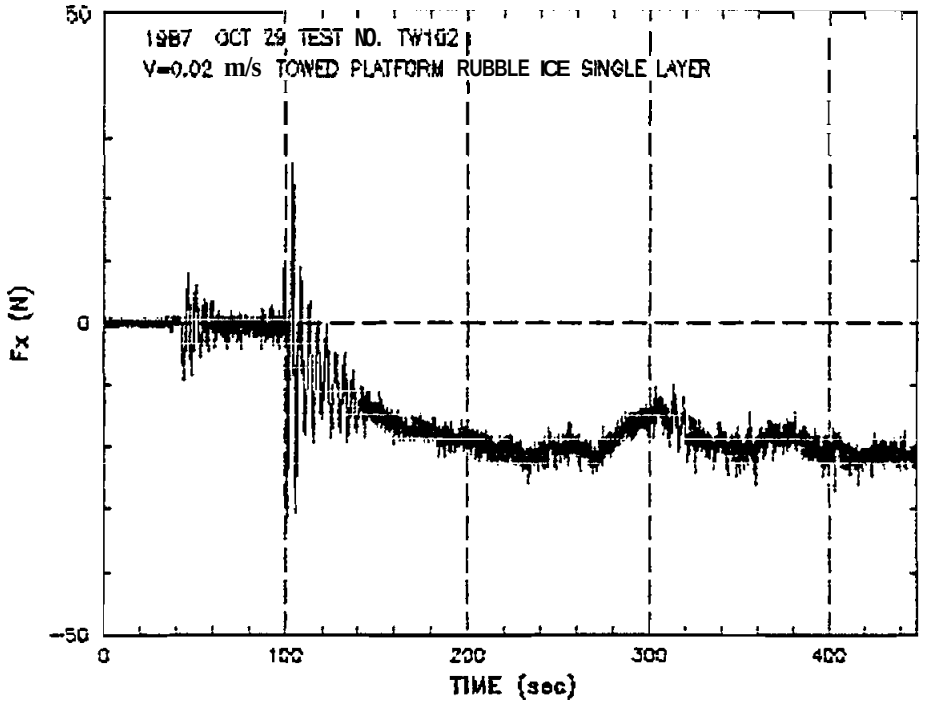


Figure 25. Surge force time history for towed platform

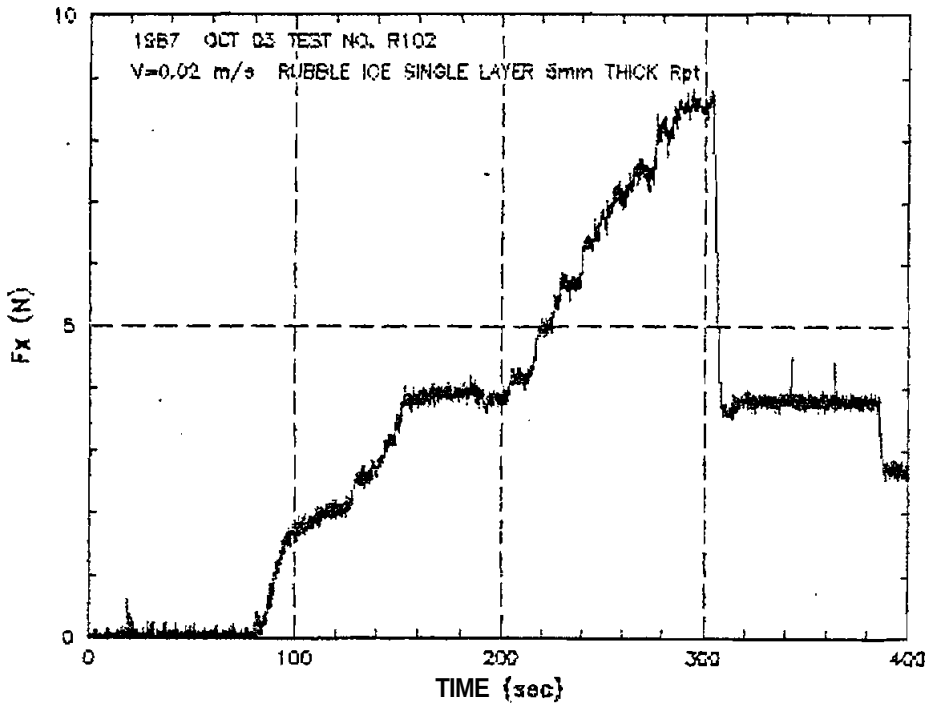


Figure 26. Surge force time history for stationary platform